SOME GENERAL PROPERTIES OF NONLINEAR REACTIVE ELEMENTS

M. D. KARASEV

Usp. Fiz. Nauk 69, 217-267 (October, 1959)

1. INTRODUCTION

AN electric resistance is considered nonlinear if its volt-ampere characteristic is nonlinear, i.e., if the current i is not proportional to the voltage u (Fig. 1). Here

$$\left.\frac{di}{du}\right|_{u=u_0} = f'(u_0) = \frac{1}{R_i} \qquad (1.1)$$

is called the differential conductance of the nonlinear resistance element and is equal in value to tan α — the slope of the volt-ampere curve at the arbitrary point $u = u_0$; R_i is correspondingly called the differential resistance. Small variations of voltage, δu, or of current, δi, are expressed approximately by the linear relation

$$\delta i \cong \frac{1}{R_i}\delta u.$$

In the absence of nonlinearity the volt-ampere characteristic becomes a straight line passing through the origin, and represents Ohm's law. Analogously, a capacitance is considered nonlinear if the charge q of the capacitor (capacitance element) depends nonlinearly on the voltage u impressed on its electrodes (Fig. 2). Small changes in the charge, δq, and in the voltage, δu, are related by the approximate linear equation

$$\delta q \cong c_i \delta u,$$
$$\left.\frac{dq}{du}\right|_{u=u_0} = f'(u_0) = c_i \qquad (1.2)$$

where c_i will be called the differential capacitance of the nonlinear capacitor. In the linear case the "volt-coulomb" characteristic of the capacitor becomes a straight line passing through the origin, and the differential capacitance C_i becomes the usual capacitance C, which is independent of the voltage.

If the distance between the capacitor electrodes does not change with changing voltage u, then the intensity of the electric field E in the capacitor is proportional to u, and the nonlinearity is due to the dependence of the dielectric constant ϵ of the capacitor dielectric on the electric field intensity E. In this case the dependences of the capacitor charge, $q = f(u)$, and of the electric induction in the capacitor, $D = \epsilon E$, on the voltage u will be

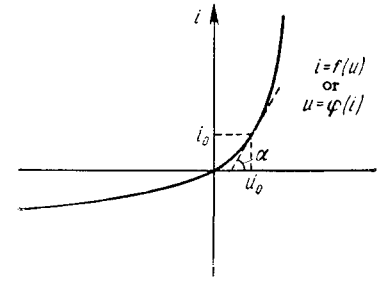

FIG. 1. Nonlinear volt-ampere characteristic of a resistance element.

similar; in a parallel-plate capacitor with homogeneous field the corresponding curves coincide upon suitable choice of scale. If the distance between the capacitor electrodes varies with the voltage, the field E is no longer proportional to the voltage but depends also on whether the plates are coming together (or apart). In this case, even if ϵ is independent of E, the connection between q and u is nonlinear, while $D = \epsilon E$ is still linear. The physical reason for this difference is that in the former case the nonlinearity is due to the displacement of the bound charges in the domain structure of the dielectric within the capacitor, and in the latter case it is due to the displacement of the free charges on the moving capacitor electrode. The commercial nonlinear "varicond" capacitor has a nonlinearity of the former type, while a diaphragm capacitor, in which the plates are elastically deflected under the influence of the mutual attraction of the electric charges on the plates, has a nonlinearity of the second type. Such diaphragm nonlinear capacitors have not found wide use in radio engineering because of the large mechanical inertia of the diaphragm. But recently, a new type of nonlinear capacitor was introduced,

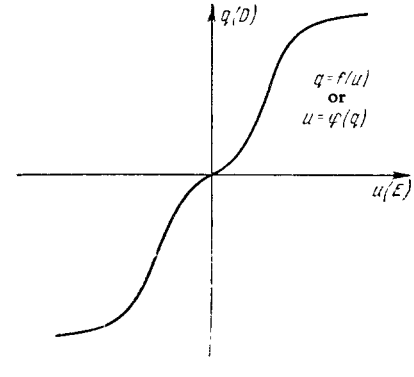

FIG. 2. Nonlinear "volt-coulomb" characteristic of a capacitor.

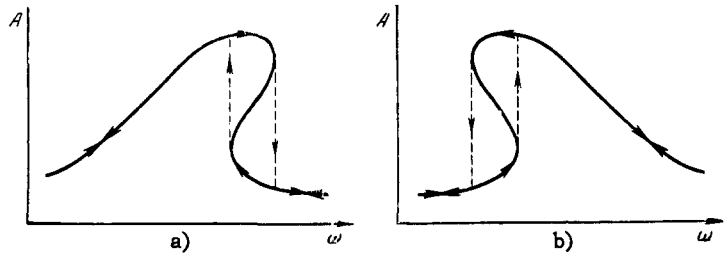

FIG. 3. Resonance curves of a tuned circuit with reactive nonlinearity. A – amplitude of the oscillations at the fundamental frequency ω; a) reactance (capacitance or inductance) decreases with increasing amplitude of oscillation; b) reactance increases with increasing amplitude of oscillations.

in which the free charges are concentrated not on metallic plates, but on both sides of a p-n junction of a transistor (see Sec. 4); this nonlinear capacitor is quite promising.

The reactive dual of the nonlinear capacitor is the nonlinear inductance, relating the magnetic flux Φ with the current i in an inductance coil. The calculations for a nonlinear capacitance can be formally employed for an inductance, provided the voltage u is replaced by the current i and the charge q by the magnetic flux Φ.

Most nonlinear problems in radio engineering involve the use of a nonlinear resistance (positive or negative). These include rectification, detection, amplitude modulation, generation of oscillations, and amplification of signals. Nonlinear reactive elements — capacitors and inductors — have come into greater use only relatively recently. This is why whatever systematic theory exists for nonlinear systems has been developed principally as applied to active nonlinearities — resistances. At the same time there are many singularities in the behavior of oscillating circuits that contain reactive nonlinearities. The principal difference between reactive and active elements is that in the former there is an accumulation and exchange of oscillation energy in electric and magnetic forms; resistances, on the other hand (whether positive or negative), can only absorb or supply energy.

We cannot say that individual properties of nonlinear reactive elements or processes in systems with nonlinear reactive elements have not been investigated at all. In fact, resonance in slightly-nonlinear oscillating circuits has been investigated rather in detail. The characteristic beak-shaped resonance curves (Fig. 3), which are accompanied by "hysteresis" phenomena (forward and backward jumps) at different frequencies, are quite well known (see, for example, reference 1).

Much attention has been paid to the parametric action on a single resonant circuit, i.e., forced variation of one of the reactive parameters of the tuned circuit. These problems which date back to the works of Melde[2] and Rayleigh,[3] have been studied in detail in the school of L. I. Mandel'shtam and N. D. Papaleksi.[4] Many important features of parametric action on an electric resonant circuit have been investigated, with account of periodic variation of one of the reactive parameters (energy pumping) as well as of the nonlinearity that limits the oscillation amplitude.

It is not our purpose to report in detail on all the investigations performed under the leadership of L. I. Mandel'shtam and N. D. Papaleksi, A. A. Andronov, A. A. Vitt, G. S. Gorelik, V. P. Gulyaev, M. A. Divil'kovskiĭ, V. A. Lazarev, V. V. Migulin, É. M. Rubchinskiĭ, S. M. Rytov, I. T. Turbovich, and others on the investigation of parametric systems. These investigations are well known. It is appropriate, however, to cite here in most concise form certain results of these investigations. In particular, the research on the parametric response of electric systems, carried out under the leadership of L. I. Mandel'shtam and N. D. Papaleksi, has established the following.

1. Periodic modulation of the capacitance or inductance of a tank circuit may give rise to oscillations. A definite relation must be satisfied here between the natural frequency ν_0 of the tank circuit (in the absence of modulation) and the modulation frequency ν. The instability accompanying the oscillations occurs at frequencies close to $2\nu_0/\nu = 1, 2, 3\ldots$ In the presence of damping in the tank circuit, furthermore, it is necessary that the depth of modulation exceed a certain minimum value, which increases with increasing number of the instability region (Fig. 4). Oscillations are easiest to produce in the first region at a modulation frequency $\nu = 2\nu_0$. A "tightening" of the re-

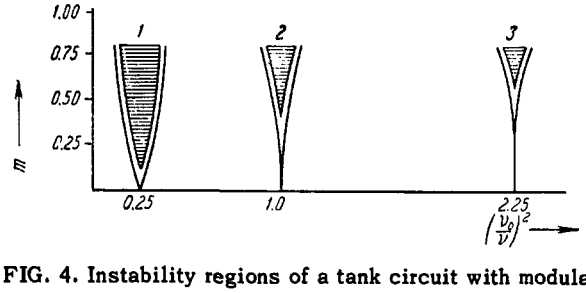

FIG. 4. Instability regions of a tank circuit with modulated reactance: 1, 2, 3. ν_0 – resonant frequency of the tank circuit in absence of modulation, ν – reactance modulation frequency; m – depth of modulation; the shaded narrowing regions of instability correspond to the presence of damping in the circuit.

sultant oscillations is observed, i.e., as the detuning is increased, the oscillations generated in the instability region cease not at the end of the instability region, but outside it; oscillations resume only upon return to the instability region. The tightening occurs on one side of the instability region, to the left or to the right, depending on the type of the reactive nonlinearity.

So-called parametric generators have been designed: capacitive, readily producing voltages up to 1500, and inductive, with a power rating up to 4 kw.[5] Certain types of parametric generators have found application in industry.

2. When a sinusoidal emf is applied to an underexcited circuit with a periodically-varying reactance, resonance is observed in the circuit. It has been established that the amplitude of the forced oscillations depends, apart from the detuning and damping of the circuit, also on the depth of modulation m of the reactance and on the phase ψ between the variation of the reactance and the applied emf. The phase dependence, which is characteristic of parametric action, manifests itself in the fact that two different types of resonance curves are obtained in two limiting cases, so called "strong" and "weak" resonance.[6] Figure 5 shows a curve for "strong" resonance under the influence of an applied emf

$$\mathcal{E} = \mathcal{E}_0 \sin(\omega t - \psi)$$

applied to a series circuit consisting of a capacitance C, a fixed resistance R, and an inductance varying as

$$L = L_0(1 + m \sin 2\omega t).$$

For comparison, Fig. 5 shows three resonance curves: A — resonance curves of the same circuit (with Q = 50) in the absence of parametric action (m = 0); B — resonance curve with increased Q (Q = 500); C — parametric resonance at $\psi = 0$ and m = 0.036. The energy is pumped into the circuit by the parametric action, through reduction in the damping. At resonance (detuning $\xi = 0$) the parametric action increases the amplitude of the oscillation by a factor

$$\frac{\frac{1}{Q}}{\frac{1}{Q} - \frac{m}{2}} = \frac{\frac{1}{50}}{\frac{1}{50} - \frac{0.036}{2}} = 10 \text{ times}.$$

However, complete equivalence with a higher-Q circuit is not observed; the bandwidth in parametric resonance is broader than that of a circuit with the corresponding value of Q.

The reverse phenomenon, that of damping of oscillations, is obtained by parametric action at "weak" resonance (Fig. 6). In this case, at a

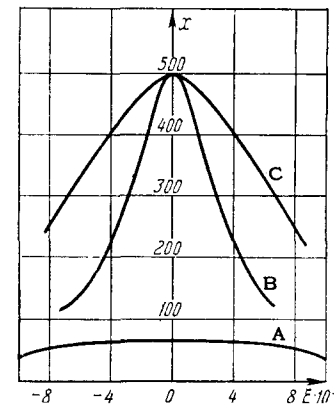

FIG. 5. Resonance curve in parametric regeneration for "strong" resonance ($\psi = 0$). $x = U_0/\mathcal{E}_0$ – ratio of the amplitude of the capacitor voltage to the amplitude of the applied emf; $\xi = \frac{\nu_0^2 - \nu^2}{\nu^2}$ is the relative detuning; ν_0 – resonant frequency of the tank circuit in the absence of modulation; ν – frequency of applied emf; 2ν – frequency of parametric action; A – resonance curve of a circuit with Q = 50 in the absence of parametric action (m = 0); B – resonance curve of a circuit with Q = 500 in the absence of parametric action; C – resonance curve of a parametrically regenerated circuit with Q = 50, depth of inductance modulation by parametric action m = 0.036.

phase shift $\psi = \pm\pi/2$, the energy, to the contrary, is removed from the resonant circuit by the parametric action, and at small detunings there is a dip in the resonance curve (curve B, Fig. 6). The same depth of modulation, m = 0.036, causes a reduction in the resonant value of the amplitude, by a factor

$$\frac{\frac{1}{Q}}{\frac{1}{Q} + \frac{m}{2}} = \frac{\frac{1}{50}}{\frac{1}{50} + \frac{0.036}{2}} = 0.54 \text{ times}.$$

As the detuning is increased, the amplitude of the forced oscillations rises sharply and becomes greater than the amplitude in the absence of para-

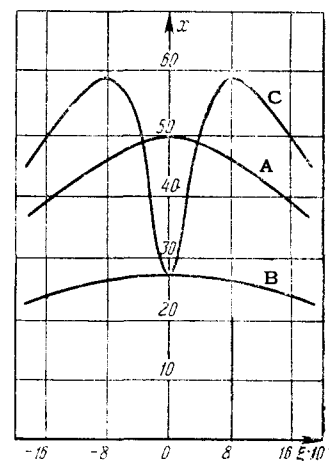

FIG. 6. Resonance curve in parametric regeneration for the case of "weak" resonance ($\psi = \pm\pi/2$). $x = U/\mathcal{E}_0$ – ratio of the capacitor voltage to the applied voltage.

metric action (curve A, Fig. 6, corresponding to m = 0 and Q = 50). The resonance curve in "weak" resonance differs greatly from the resonance curve of a circuit with Q correspondingly reduced (by a factor 0.54) (B in Fig. 6).

It has been shown in reference 6 that synchronous action at double the frequency on the reactive parameter of a tank circuit is analogous to feedback (positive when $\psi = 0$ or negative when $\psi = \pi/2$), and that such a system represents a special type of parametric regenerative amplifier.

"Strong" resonance can lead to undamped natural oscillations, if m/2 becomes greater than 1/Q. However, a mathematical analysis of this mode discloses qualitative differences. As early as in 1933, Mandel'shtam and Papaleksi[7] have shown that the launching of parametrically excited oscillations can be explained only by a nonlinear theory. Such a nonlinear theory was then developed by Mandel'shtam and Papaleksi.* On the other hand, processes in underexcited parametric regenerative circuits can be described rather completely by means of linear equations with variable coefficients. In investigating the parametrically regenerative systems, Soviet radio physicists have established many other properties of such systems. In particular, G. S. Gorelik[8] has shown that whereas the simplest types of oscillations in resonant systems with constant parameters are sinusoidal and that such systems produce harmonic oscillations at resonance, the simplest oscillations for a parametric regenerative system will be not sinusoidal, but represented by other functions, which depend on the character of the variation of the system parameter with time. If a sinusoidal emf is applied to a parametric regenerative system, the system resolves this oscillation into the eigenfunctions inherent in that system, just as a resonant system with fixed parameters realizes the spectral analysis of a complex oscillation into its harmonic components. Thus, the concept of resonance was generalized to include linear oscillating circuits with periodically-varying parameters.

L. I. Mandel'shtam attached very great significance to systems with variable parameters. Unfortunately, he was unable to finish the projected monograph on parametric generation of alternating currents; the preparatory notes for this monograph were published posthumously.[9] Mandel'shtam proposed to consider in this monograph the general laws of a system with variable parameters and many degrees of freedom; this analysis would include ordinary dynamos and electrostatic generators in a natural manner as degenerate systems, in which the electric or magnetic energy respectively is negligibly small; he proposed to define as "non-degenerate parametric generators" those in which both types of energy, magnetic and electric (or, in general, kinetic and potential), play a substantial role simultaneously, and in which oscillations are excited when definite relations obtain between the periods of variation of the parameters and the magnitudes of the parameters themselves.

V. V. Migulin, who participated together with V. P. Gulyaev, V. A. Lazarev, and others in work on the study of parametric actions on electric systems, carried out in the Thirties at the Leningrad Electrophysics Institute under the leadership of N. D. Papaleksi, was kind enough to report to us that as early as 1934, the investigations concerned not only single-circuit systems, but also two-circuit parametric systems. The possibility of parametric excitation at frequencies noncommensurate with the frequency of parametric action were also studied. In a paper[10] published in 1939, Papaleksi describes parametric interaction in a two-circuit electromechanical system (consisting of an electric oscillating circuit and a parametric motor) in response to a difference frequency. He notes in conclusion of his article that the parametric action in such a system "yields a new unique frequency transformation at practically any frequency ratio." He thus disclosed, as early as in the Thirties, the possibility of parametric action not only at multiple frequencies, but also at non-commensurate frequencies. However, the lack of technical facilities in those days (and also the absence of a definite need) for a broader utilization of these phenomena did not stimulate a deeper study.

Recently new interest in variable reactive elements has been generated in connection with possible use in the microwave range. But they deserve great attention for their own sake, from the point of view of development of a general theory of nonlinear oscillations. Variable reactive elements have properties that are both similar to and different from those of variable resistances. Thus, a nonlinear capacitance or a nonlinear inductance is capable of generating harmonics, just as a nonlinear resistance. Apparently, the development of high-Q nonlinear reactive elements for microwaves is rapidly displacing nonlinear resistances

*The nonlinear theory of self-oscillating systems (including those with nonlinear reactances) was subsequently developed in the papers of K. F. Teodorchik for certain types of systems and reduced to a simple and lucid form by the so-called energy methods. Автоколебательные системы (Self-oscillating Systems), M., 1952.

(which are inherently lossy) from all microwave apparatus used for generating very high frequencies by frequency multiplication.

In the rectification of alternating current, a nonlinear element is also essential. But in this case the nonlinear element must be a nonlinear resistance. It is impossible to obtain dc from ac by means of a purely reactive element, even a nonlinear one. Let us assume, for the sake of being specific, that a saturable reactor is used as a nonlinear reactance element and that the electric circuit is as shown in Fig. 7. A direct voltage E produces the initial magnetizing direct current, and an alternating emf without a dc component [$\mathscr{E}(t) = \mathscr{E}(t+kT_0)$, where T_0 is the period], forces the flow of alternating current in the circuit. The internal resistance of the two voltage sources, as well as the internal resistance of the inductance coil, will be lumped with that of resistor R, the load. In the absence of an alternating voltage, only direct current will flow in the circuit, and its value will obviously be

$$i_0 = \frac{E}{R}.$$

As a result of simultaneous action of E and $\mathscr{E}(t)$ (which are not equal to 0), there will be established eventually in the circuit of Fig. 7 a periodic current, which can be presented as

$$i(t) = I_0 + \sum_{n=1}^{\infty} I_n \cos\left(2\pi \frac{n}{T_1} t + \varphi_n\right), \qquad (1.3)$$

where I_0 is the dc component, I_n the amplitude of the n-th harmonic, T_1 the shortest period of current oscillation, which in general can be a multiple or rational-fraction of T_0, i.e., $T_1 = (p/q)T_0$. It is obvious that were rectification possible, we would have

$$I_0 \neq i_0. \qquad (1.4)$$

Let us find the value of I_0. For this purpose we consider the fact that the periodic current (1.3) excites in the inductance coil a nonlinear, but also periodic, magnetic flux

$$\Phi(i) = \Phi(t + kT_1),$$

determined by the connection between the ampere turns of the coil and its magnetic flux. The equation of the circuit shown in Fig. 7 is of the form

$$\mathscr{E}(t) + E = Ri(t) + n\frac{d\Phi}{dt}. \qquad (1.5)$$

If we now find the mean value of the right and left sides of (1.5) over an infinitely large time interval, we obtain the sought value of I_0 as the limit

$$\lim_{T\to\infty}\left\{\frac{1}{T}\int_t^{t+T}(\mathscr{E}(t)+E)\,dt = \frac{1}{T}\int_t^{t+T}\left(Ri(t)+n\frac{d\Phi}{dt}\right)dt\right\}. \qquad (1.6)$$

FIG. 7. Nonlinear circuit with a saturable reactor.

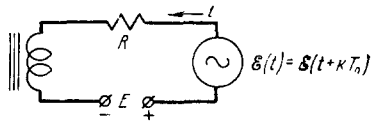

From (1.6) we get $E = RI_0$, i.e., $I_0 = i_0$. From this condition, which contradicts condition (1.4), it follows that it is impossible to rectify with an inductance.

This premise is supplemented by its converse: it is impossible to invert direct current into periodic alternating current by means of a system consisting of any combination of nonlinear reactive elements and fixed resistances. It is known that any amplifier, in the presence of positive feedback and at sufficiently high gain, can become a generator of undamped oscillations. The question arises: is it possible to produce a system comprising magnetic or dielectric amplifiers, fed from a dc source, capable by itself of converting the direct current into alternating current with the aid of nonlinear reactive elements? The answer is no.

This can be demonstrated in the following manner. Assume that we have a passive nonlinear two-port network, containing any finite number of fixed resistances R_k, nonlinear capacitors with differential capacitances C_l, and inductance coils with differential inductances L_m, interconnected in any manner. We connect a direct voltage E to the input of this network, and connect a fixed load resistance R_L across the output terminals, as shown in Fig. 8.

FIG. 8. Passive two-port network containing nonlinear reactive elements.

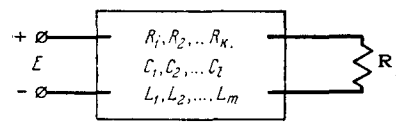

Let us ascertain the number of equilibrium states of the circuit of Fig. 8. In equilibrium, all the currents in a circuit and all the voltage across each element are constant. But the capacitor, as a pure reactance, is an infinite resistance — an open circuit — to direct current, and an inductance is likewise a short circuit to direct current. Consequently, the two-port network shown in Fig. 8 is equivalent, in its equilibrium state, to a combination of resistors R_k only, with open circuits where the capacitors are connected and short circuits where the coils are connected. But in a circuit consisting of fixed resistors, there can be only one value of current and voltage for each network element in response to a specified direct voltage. Thus, the circuit of Fig. 8 has only one equilibrium position.

If this only equilibrium position is unstable, then self-oscillations are possible in the system and alternating current can be generated; if the

equilibrium is stable, no alternating current can be excited.

To determine whether the equilibrium is stable we must examine the response of the system to small changes in all currents and voltages near the equilibrium values, assuming the capacitors and inductors to be constant. The equilibrium is unstable if at least in one of the loops small disturbance produces an increasing deviation of the current or voltage from equilibrium value. Referring to the nonlinear characteristics of the reactive elements q(u) and Φ(i) (see Fig. 2), we note that they have the distinguishing feature that although the differential capacitance and differential inductance are not constant, i.e., they depend on the voltage or current, they cannot be negative. In this respect they differ qualitatively from a nonlinear resistance, the differential values of which can be negative. For example, in certain phases of a gas discharge, an increase in the discharge-gap current causes so large an increase in conductance by ionization, that the voltage drop across the gap decreases, in spite of the increased current; in this case the differential resistance of the gap is negative. But the charge q of a capacitor or the magnetic field Φ in an inductor cannot decrease with increasing electric or magnetic field; the dielectric constant or the permeability cannot be negative.*

A negative resistance can be produced artificially by using dc sources and negative feedback to control the conductivity. For example, it is easy to obtain in a pentode, through the transitron effect, a portion of the characteristic with a negative resistance between the screen grid and the cathode, by applying a portion of the potential from the screen grid to the suppressor (pentode) grid (Fig. 9).† In this case control of conductance by feedback is accompanied by energy loss only in the external control circuit (in the resistors of voltage divider R_1R_2, Fig. 9), and the total energy that the section with the negative resistance can supply exceeds the energy necessary to control the feedback. Only under this condition is a negative resistance produced. In nonlinear reactive elements it is also possible to use feedback, for example, by using additional windings in the inductance coils. But in reactive elements the currents and voltages are related respectively with the magnetic and

*This does not contradict the fact that the dielectric constant or magnetic permeability can be less than unity. For example, in the substance with the most clearly pronounced diamagnetism, bismuth, $\mu - 1 = -8\pi \times 10^{-5}$. Superconductors can be likened to substances with $\mu = 0$.

†See K. F. Teodorchik, loc. cit., p. 152.

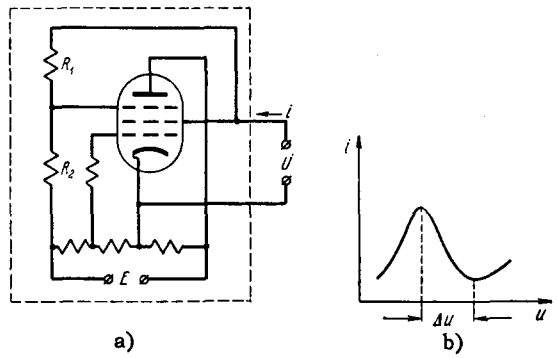

FIG. 9. One-port network with negative differential resistance: a – electronic circuit, b – volt-ampere characteristic.

electric energy. It can be shown that the feedback in this case requires the consumption of so much power, that the effect of the negative reactive resistance is fully balanced by the positive damping due to energy loss in the feedback circuit. Assume, for example, that we have succeeded in obtaining, by using feedback, a section with a negative differential capacitance. It will be characterized by a capacitor q vs. u curve that has a negative slope (Fig. 10). Assume now that the capacitor voltage has increased by Δu (from a value u_0 to $u_0 + \Delta u$). Then the capacitor charge, in accordance with the characteristic shown in Fig. 10, will decrease by Δq (from q_0 to $q_0 - \Delta q$), and the energy delivered to the external circuit will be

$$\Delta W_{\text{out}} \cong u_0 \Delta q. \tag{1.7}$$

But in this case the reduction in the capacitor energy is not greater than half the value of (1.7), being equal to

$$\Delta W_{\text{cap}} \cong -\frac{1}{2} u_0 \Delta q + \frac{1}{2} q_0 \Delta u. \tag{1.8}$$

The value of (1.8) equals half of ΔW_{out}, with the opposite sign, for an infinitely large negative differential capacitance

$$\Delta W_{\text{cap}} \cong -\frac{1}{2} u_0 \Delta q \quad \text{for} \quad \frac{dq}{du} = \infty.$$

On the other hand, if dq/du ≅ 0, then

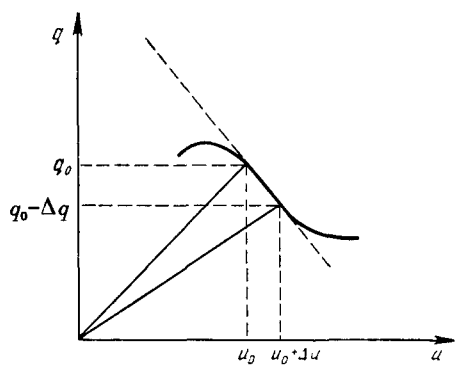

FIG. 10. Characteristic of nonlinear capacitance with a section having a negative differential capacitance.

$$\Delta W_{\text{cap}} \cong \frac{1}{2} q_0 \Delta u > 0,$$

i.e., the capacitor energy increases with the voltage applied to it. Consequently, more than half of the energy delivered to the external circuit by the negative capacitance will always be drawn from the feedback circuits. Thus, even under optimum matching, not more than one-half of the total power can be drawn from any source. It follows therefore that it is impossible to construct a negative capacitance with internal feedback only, capable of pumping energy into an external circuit without any external alternating voltage sources.

Returning to the equilibrium state in our two-port network of Fig. 8, we see that the equilibrium is stable, for all the reactive elements contained in the two-port network are positive and when used in conjunction with positive resistances cannot lead to increasing solutions near the equilibrium position.

The foregoing features of nonlinear reactive elements, which distinguish them sharply from the nonlinear resistances used in rectification and generation of alternating current, are quite remarkable. They are found to agree with the rather general relations derived by Manly and Rowe[11] in 1956. The next section will be devoted to an analysis of these relations, which describe the flow of energy in a system containing a nonlinear reactance.

2. GENERAL ENERGY RELATIONS FOR NONLINEAR REACTIVE ELEMENTS

Nonlinear reactive elements are used most extensively as modulators in magnetic and dielectric amplifiers. In this case voltages of two different frequencies are applied to the nonlinear reactance — the signal and the amplifier power supply. The effect of amplification is to change, by means of the input signal, the energy flowing into the load. Let us consider the behavior of a nonlinear hysteresis-free capacitance, under the influence of two emfs of different (in general, non-commensurate) frequencies ν_0 and ν_1.

Let the relationship between the charge q and the voltage u across a nonlinear capacitance be given by the single-valued function

$$u = \varphi(q). \tag{2.1}$$

No additional assumptions are made concerning the form of the nonlinearity of (2.1), except for absence of hysteresis or losses, i.e., except that the element is considered to be purely reactive. The charge in the nonlinear capacitance will vary under the influence of the two periodic emfs with frequencies ν_0 and ν_1. In the steady state the change in charge will include, generally speaking, various arbitrary combination frequencies $m\nu_0 + n\nu_1$, but no other frequencies will be contained in the spectrum of charge oscillations. With this consideration, we can represent the charge q formally by means of the complex double Fourier series in the combination frequencies $m\nu_0 + n\nu_1$

$$q(t) = \sum_{m=-\infty}^{+\infty} \sum_{n=-\infty}^{+\infty} \dot{Q}_{m,n} e^{j(mx+ny)}, \tag{2.2}$$

where $x = \omega_0 t$, $\omega_0 = 2\pi\nu_0$; $y = \omega_1 t$, and $\omega_1 = 2\pi\nu_1$. Since q(t) is real, we have

$$\dot{Q}_{m,n} = \dot{Q}^*_{-m,-n}$$

(the asterisk denotes complex conjugation).

If the frequencies ν_0 and ν_1 are not commensurate, q(t) may be nonperiodic, but the series (2.2) retains its meaning; this double series of the single variable t will accordingly contain components with non-commensurate frequencies.

Thus, the change in charge q(t) is represented by a set of discrete harmonic oscillations with frequencies $m\nu_0 + n\nu_1$; the respective complex amplitude of each harmonic component will be $\dot{Q}_{m,n}$. From this we can readily obtain the complex amplitude of the current at the corresponding frequency

$$\dot{I}_{m,n} = j(m\omega_0 + n\omega_1)\dot{Q}_{m,n}, \tag{2.3}$$

and the current i(t) will be expressed by an analogous double Fourier series

$$i(t) = \frac{dq}{dt} = \sum_{m=-\infty}^{+\infty} \sum_{n=-\infty}^{+\infty} \dot{I}_{m,n} e^{j(mx+ny)}. \tag{2.4}$$

As in the case of the charge, we have

$$\dot{I}_{m,n} = \dot{I}^*_{-m,-n}.$$

Using (2.1), we can also represent the voltage u(t) across the nonlinear capacitance by a double Fourier series

$$u(t) = \varphi\{q[x(t), y(t)]\} = F(x, y), \tag{2.5}$$

$$u = \sum_{m=-\infty}^{+\infty} \sum_{n=-\infty}^{+\infty} \dot{U}_{m,n} e^{j(mx+ny)},$$

$$\dot{U}_{m,n} = \dot{U}^*_{-m,-n}. \tag{2.6}$$

As already indicated, the double Fourier series is derived formally. The determination of the coefficients may entail in general a tremendous amount of calculation. As will be shown later, important conclusions can be drawn even without performing any computation, i.e., without specifying the type of function (2.1) and the type of network in which the nonlinear reactance is used.

With the aid of known integral forms we can

express formally all the coefficients of the foregoing Fourier series. In particular, the coefficients of series (2.6) are

$$\dot{U}_{m,n}=\frac{1}{(2\pi)^2}\int_0^{2\pi}dy\int_0^{2\pi}dx\,F(x,y)\,e^{-j(mx+ny)}. \quad (2.7)$$

Let us multiply (2.7) by $jmQ^*_{m,n}$ and sum the resultant terms over n and m from $-\infty$ to $+\infty$. Then, interchanging the order of integration and summation on the right side we obtain

$$\sum_{m=-\infty}^{+\infty}\sum_{n=-\infty}^{+\infty}jm\dot{Q}^*_{m,n}\dot{U}_{m,n}$$

$$=\frac{1}{(2\pi)^2}\int_0^{2\pi}dy\int_0^{2\pi}dx\,F(x,y)\sum_{m=-\infty}^{+\infty}\sum_{n=-\infty}^{+\infty}jm\dot{Q}^*_{m,n}e^{-j(mx+ny)}. \quad (2.8)$$

Differentiating (2.2) with respect to x we get

$$\frac{\partial q}{\partial x}=\sum_{m=-\infty}^{+\infty}\sum_{n=-\infty}^{+\infty}jm\dot{Q}_{m,n}e^{j(mx+ny)}. \quad (2.9)$$

Making use of the equality of complex-conjugate coefficients whose indices have opposite signs, we can rewrite (2.9) as

$$\frac{\partial q}{\partial x}=-\sum_{m=-\infty}^{+\infty}\sum_{n=-\infty}^{+\infty}jm\dot{Q}^*_{m,n}e^{-j(mx+ny)}. \quad (2.9')$$

The expression (2.9') taken with a negative sign is identical with the expression under the double sum in the right half of (2.8). Using (2.3) and replacing in it $\dot{Q}_{m,n}$ by the complex conjugate after inserting (2.8) in the left half, we obtain

$$\sum_{m=-\infty}^{+\infty}\sum_{n=-\infty}^{+\infty}\frac{m\dot{U}_{m,n}\dot{I}^*_{m,n}}{m\nu_0+n\nu_1}=\frac{1}{2\pi}\int_0^{2\pi}dy\int_0^{2\pi}dx\,\frac{\partial q}{\partial x}F(x,y). \quad (2.10)$$

The expression $\frac{\partial q}{\partial x}dx$ is equal to dq when y = const. Taking this into account, we rewrite (2.10) in the form

$$\sum_{m=-\infty}^{+\infty}\sum_{n=-\infty}^{+\infty}\frac{m\dot{U}_{m,n}\dot{I}^*_{m,n}}{m\nu_0+n\nu_1}=\frac{1}{2\pi}\int_0^{2\pi}dy\int_{q(0,y)}^{q(2\pi,y)}\varphi(q)\,dq. \quad (2.11)$$

The limits of the second integral on the right half of (2.11) show that the change in q is determined by the change in x from 0 to 2π at constant y.

Interchanging the roles of x and y, we can obtain relations analogous to (2.8) — (2.11), and, in particular,

$$\sum_{m=+\infty}^{+\infty}\sum_{n=-\infty}^{+\infty}\frac{n\dot{U}_{m,n}\dot{I}^*_{m,n}}{m\nu_0+n\nu_1}=\frac{1}{2\pi}\int_0^{2\pi}dx\int_{q(x,0)}^{q(x,2\pi)}\varphi(q)\,dq, \quad (2.12)$$

where the integration variable in the second integral changes as y changes from 0 to 2π and x remains constant.

We now introduce the energy characteristics of the harmonic components of the current and voltage in the reactance. We denote by $P_{m,n}$ a quantity proportional to the average active power at the frequency $m\nu_0+n\nu_1$,

$$P_{m,n}=\dot{U}_{m,n}\dot{I}^*_{m,n}+\dot{U}^*_{m,n}\dot{I}_{m,n}=P_{-m,-n}, \quad (2.13)$$

and by $X_{m,n}$ a quantity proportional to the reactive power at the same frequency

$$jX_{m,n}=\dot{U}_{m,n}\dot{I}^*_{m,n}-\dot{U}^*_{m,n}\dot{I}_{m,n}=-jX_{-m,-n}. \quad (2.14)$$

Then the complex power at the combined frequency $m\nu_0+n\nu_1$ will be proportional to

$$\dot{S}_{m,n}=P_{m,n}+jX_{m,n}=2\dot{U}_{m,n}\dot{I}_{m,n}=\dot{S}^*_{-m,-n} \quad (2.15)$$

Turning now to (2.11) and (2.12), we can readily verify that the right halves contain only active power components, (2.13), and do not contain the reactive power (2.14) at all. Actually, if, for example, we group the components in the double sum of the left half of (2.11) in pairs with opposite signs of m and take the complex conjugate of the coefficients with negative indices, we obtain

$$\sum_{m=0}^{+\infty}\sum_{n=-\infty}^{+\infty}\frac{mP_{m,n}}{m\nu_0+n\nu_1}=\frac{1}{2\pi}\int_0^{2\pi}dy\int_{q(0,y)}^{q(2\pi,y)}\varphi(q)\,dq. \quad (2.11')$$

Analogously, we obtain from (2.12)

$$\sum_{m=-\infty}^{+\infty}\sum_{n=0}^{+\infty}\frac{nP_{m,n}}{m\nu_0+n\nu_1}=\frac{1}{2\pi}\int_0^{2\pi}dx\int_{q(x,0)}^{q(x,2\pi)}\varphi(q)\,dq. \quad (2.12')$$

In Eqs. (2.11) and (2.12') the summation is over different domains; $P_{m,n}$ represents the mean active power in the nonlinear capacitance at frequencies $\pm[m\nu_0+n\nu_1]$. To recast the left halves of (2.11') and (2.12') in identical form, they must be rewritten so that the denominators contain only positive frequencies, and the indices of P have the corresponding values with allowance for relation (2.13). For example, the term of frequency $3\nu_0-2\nu_1$ (if $3\nu_0>2\nu_1$) in (2.11') has the form

$$\frac{3P_{3,-2}}{3\nu_0-2\nu_1}.$$

The term of the same frequency is written in (2.12') as

$$\frac{2P_{-3,+2}}{-3\nu_0+2\nu_1}=-\frac{2P_{+3,-2}}{3\nu_0-2\nu_1}.$$

Since q is periodic both in x and in y in the steady state, the uniqueness of (2.1) leads to the vanishing of the integrals from 0 to 2π over x and over y in the right halves of (2.11') and (2.12). In final form, the energy relations for a nonlinear capacitance have the form

$$\sum_{m=0}^{+\infty}\sum_{n=-\infty}^{+\infty}\frac{mP_{m,n}}{m\nu_0+n\nu_0}=0, \quad (2.16)$$

$$\sum_{m=-\infty}^{+\infty}\sum_{n=0}^{+\infty}\frac{nP_{m,n}}{m\nu_0+n\nu_1}=0. \qquad (2.17)$$

The vanishing of the right halves of (2.11′) and (2.12′) means that on the average energy can be neither accumulated nor consumed by a capacitance in the steady state. Equations (2.16) and (2.17) establish the energy distribution over the combination frequencies. The remarkable fact is that regardless of the type of nonlinearity and the type of energy-consuming device, the power distribution over the combination frequencies depends on the magnitudes and signs of the combination frequencies. This is formally reminiscent of the quantum energy relations, where the energy quantum is proportional to the frequency.*

Since in the absence of hysteresis no energy can be consumed in a nonlinear reactance, the power summed over all frequencies should vanish. This result is obtained by multiplying (2.16) by ν_0, (2.17) by ν_1, and adding.

Equations (2.16) and (2.17) should hold also for linear reactances, i.e., for constant C and L. There is no modulation in a fixed capacitance, nor are there combination frequencies. Only one term, $P_{1,0}/\nu_0 = 0$ remains in Eq. (2.16), while the only term remaining in (2.17) is $P_{0,1}/\nu_1 = 0$, as should be.

We have assumed from the very outset that two sources, with frequencies ν_0 and ν_1, are connected to the device with the reactive nonlinearity. Consequently, energy can be fed to this device only from these sources, and all the $P_{m,n}$ should be negative, with the exception of $P_{1,0}$ and $P_{0,1}$, which represent the power flowing from the sources to the device. Since (2.16) contains $P_{1,0}$ and does not contain $P_{0,1}$ (m = 0), and the reverse holds for (2.17), these two equations are resolved for the corresponding generators in terms of sideband-frequency powers.

Equations (2.16) and (2.17) make it possible, without investigating the network in detail, to answer two important questions concerning the operation of a device with reactive nonlinearity: they furnish an estimate of the maximum power gain and an estimate of the stability.

To illustrate the use of Eqs. (2.16) and (2.17), let us consider a simple but important case, of a modulator or demodulator with only one combination frequency $\nu_0 + \nu_1$ (or $\nu_0 - \nu_1$). We assume the remaining combination frequencies to be suppressed by ideal lossless filters.

Thus, let a signal frequency ν_1 and a carrier frequency ν_0 be applied to a nonlinear capacitance from two generators. Let furthermore $\nu_0 > \nu_1$.

*See M. T. Weiss, Proc. IRE, 45, No. 7, 1012 (1957).

We consider first the so-called non-inverted case of modulation, when the combination frequency is $\nu_0 + \nu_1$.*

In the non-inverted case (2.16) and (2.17) yield:

$$\frac{P_{1,0}}{\nu_0}+\frac{P_{1,1}}{\nu_0+\nu_1}=0, \qquad (2.18)$$

$$\frac{P_{0,1}}{\nu_1}+\frac{P_{1,1}}{\nu_0+\nu_1}=0. \qquad (2.19)$$

In the modulator circuit, the energy flows from the generator at the carrier frequency ν_0; consequently, $P_{1,0}$ is positive. The power flowing into the load is at the combination frequency $\nu_0 + \nu_1$; this power $P_{1,1}$ flowing from the nonlinear reactance to the load, will be considered negative. Equation (2.18) shows that the energy flow into the load exceeds somewhat the flow from the carrier generator

$$P_{1,1}=-P_{1,0}\frac{\nu_0+\nu_1}{\nu_0}.$$

Some of the signal-generator energy is also used to control the modulator. It follows from (2.19) that $P_{0,1}$ is positive. The ratio of the output power $-P_{1,1}$ to the signal input power, $P_{0,1}$, determines the power gain of the non-inverted modulator

$$G_+=-\frac{P_{1,1}}{P_{0,1}}=\frac{\nu_0+\nu_1}{\nu_1}. \qquad (2.20)$$

A non-inverted modulator is always stable. The gain G_+ increases with increasing carrier frequency (relative to the signal frequency). If, to the contrary, a modulated signal with combination frequency $\nu_0 + \nu_1$ is applied to the reactive nonlinearity together with the carrier, we obtain a demodulator. The positive power will be $P_{1,1}$, and the other two will be negative. The gain of the demodulator will be the reciprocal of (2.20), i.e., less than unity. The energy of the modulated signal will be partially directed towards the load and will flow for the most part to the carrier generator. If the modulated-signal source is sufficiently powerful, the circuit may become unstable because of the negative resistance introduced by the demodulator in the output of the carrier generator. The operation of a non-inverted modulator or demodulator is illustrated in Fig. 11.

As indicated in the introduction, reference 10 considered a two-loop electromechanical circuit, consisting of an electric resonant network and a parametric motor. This circuit was fed with a sinusoidal voltage of frequency ω, and the network was tuned to a frequency close to ω_ν, while the inductance in the parametric motor was varied at a frequency $\omega_p = \omega - \omega_\nu$ (the notation is that

*The total modulation is called non-inverted because the frequency band of the anharmonic modulating oscillation is merely shifted towards the higher frequencies, while in the case of differential modulation this band is also mirror-inverted.

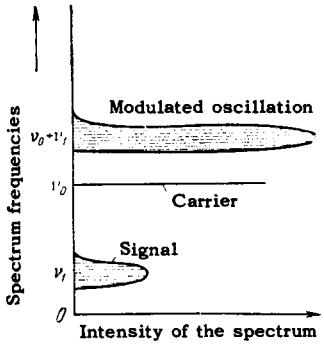

FIG. 11. Illustration of the operation of a non-inverting modulator and demodulator. The two lower levels ν_0 and ν_1 are in balance with the upper level $\nu_0 + \nu_1$.

of reference 10). Thus, the energy was fed to this parametric network at a frequency $\omega = \omega_p + \omega_\nu$, and was consumed in part at a frequency ω_p in the motor (ω_p is a multiple of the angular velocity of the motor) and in part at a frequency ω_ν in the resonant circuit. By varying the natural frequency ω_ν of the resonant circuit, the speed of the parametric motor can be varied over a very wide range, from a very low value up to ω. In our terms, this circuit is similar to a demodulator; ω corresponds to $\nu_0 + \nu_1$, the frequency ω_ν of the resonant circuit corresponds to ν_1, and the parameter frequency ω_p corresponds to ν_0.

Let us consider now an inverting modulator, in which ideal filters are used to suppress all the combination frequencies, with the exception of the differential frequency $\nu_0 - \nu_1$. Equations (2.16) and (2.17) yield in this case

$$\frac{P_{1,0}}{\nu_0} + \frac{P_{1,-1}}{\nu_0 - \nu_1} = 0, \tag{2.21}$$

$$\frac{P_{0,1}}{\nu_1} - \frac{P_{1,-1}}{\nu_0 - \nu_1} = 0. \tag{2.22}$$

It follows from (2.21) that not all the energy supplied by the carrier generator flows into the load

$$-P_{1,-1} = +P_{1,0}\frac{\nu_0 - \nu_1}{\nu_0} < P_{1,0}.$$

Equation (2.22) shows that the signal power $P_{0,1}$ and the modulated output power $P_{1,-1}$ have the same sign, i.e., no signal power is needed for control of the modulator in this case but, to the contrary, the modulator adds to the signal-power frequency. The inverting modulator introduces a negative resistance to the output circuit of the signal generator and is thus potentially subject to instability. The gain, according to (2.2) is negative:

$$G_- = \frac{-P_{1,-1}}{P_{0,1}} = -\frac{\nu_0 - \nu_1}{\nu_0} < 0. \tag{2.23}$$

The input signal circuit always produces losses. These losses can be offset to a greater or lesser degree by the power fed to the input circuit. If the energy flowing from the nonlinear reactance to the signal circuit exceeds the loss in the circuits, stability is lost and the modulator becomes self-oscillating. The inverting modulator does not operate in the ordinary manner; the only way that carrier power can be produced is by applying both the modulated oscillation and the signal itself to the demodulator. The operation of the inverting modulator is illustrated in Fig. 12.

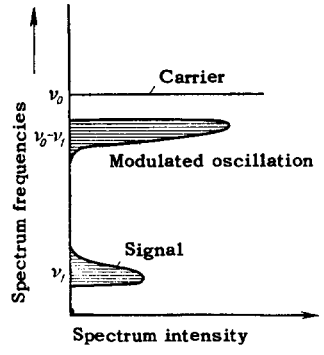

FIG. 12. Illustration of the operation of an inverting modulator. The two levels, ν_1 and $\nu_0 - \nu_1$ are in balance with the upper level ν_0.

In an ordinary magnetic amplifier both the upper and the lower sideband frequencies are retained, and therefore the energy relations are more complicated. But it is clear from the foregoing analysis that the magnetic amplifier can lose stability and become excited at a certain low frequency, at which the power delivered to the signal circuit through the lower sideband of the modulated oscillations in the output circuit will exceed the losses. Obviously, such a coincidence of circumstances gave rise to the self-oscillation of the magnetic modulator described in reference 12.

The following basic question suggests itself: what limits the amplitude of the self-oscillations produced when the modulator becomes unstable? We imposed no limitations on the signal amplitude or on the type of the reactive nonlinearity in the derivation of the relations (2.16) and (2.17). At the same time, the energy relations do not contain the type of nonlinearity in explicit form. From the nature of the analysis of the operation of a nonlinear reactance, carried out in this section, it follows that the nonlinearity of the reactance is considered only as a "generator" of combination frequencies. The greater the nonlinearity, the easier it is to launch the combination-frequency oscillations, but since the reactance involves no loss, the power balance over all the combination frequencies will be strictly maintained. In the self-excitation of an inverting modulator the situation is the following. At first the oscillations build up and their intensity increases simultaneously in the signal and output circuits. The carrier generator develops in this case more and more power. Assuming that the circuit contains only one reactive nonlinearity, the oscillations

are limited by the internal resistance of the carrier generator. In fact, an increase in intensity of the oscillation at the frequencies ν_1 and $\nu_0 - \nu_1$ is accompanied by an increase in the power drawn from the carrier generator at ν_0, and this is equivalent to a reduction in the load resistance of this generator. In final analysis, the power delivered to the nonlinear reactance from the carrier generator is limited by internal resistance of this generator. Assuming that the equivalent load resistance R_{eq}, seen by the carrier generator diminishes in proportion to the summary intensities of the oscillations at ν_1 and $\nu_0 - \nu_1$, i.e.,

$$\frac{1}{R_{eq}} \sim |P_{0,1} + P_{1,-1}|,$$

and considering that

$$|P_{0,1} + P_{1,-1}| = P_{1,0},$$

then the intensity of the steady-state oscillations can be obtained from the graph shown in Fig. 13. Generally speaking, the establishment of the steady state oscillations is influenced by the losses in the nonlinear reactance, which we do not take into account and which depend in a complex manner on the frequency and intensity of the oscillations. These losses may modify significantly the mechanism proposed here for the limitation self-oscillations.

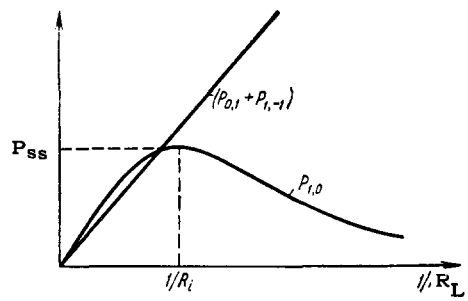

FIG. 13. Establishment of self-oscillations in a self-excited inverting modulator: $P_{0,1} + P_{1,-1}$ – power of generated self-oscillations; $P_{1,0}$ – power drawn from the carrier generator; P_{ss} – steady-state power; R_i and R_L – internal resistance of the carrier generator and equivalent resistance of its load.

Attention should be called to still another fact about the general power relations. When either the nonlinearity of the reactive element or the intensity of the oscillations is large, complete suppression of all the combination frequencies, with the exception of a few chosen ones (say with the exception of ν_1 and $\nu_0 - \nu_1$), is possible, strictly speaking, only with the aid of infinitesimally narrow filters. We readily see that at sufficiently large values of m and n, the difference between ν_1 and $|m\nu_0 + n\nu_1|$ or between $\nu_0 - \nu_1$ and $|m\nu_0 + n\nu_1|$ can become sufficiently small, provided the approximate equality

$$\frac{n \pm 1}{m} \cong -\frac{\nu_0}{\nu_1}$$

or

$$\frac{n \pm 1}{m \mp 1} \cong -\frac{\nu_0}{\nu_1}.$$

is satisfied. If the filters have finite bandwidths, the amplitudes of these combination frequencies of higher numbers will not be suppressed and a considerable redistribution of the power will result. Since high nonlinearity of the reactive element or high intensity of oscillation makes the amplitude of the higher combination frequencies commensurate with the amplitudes of ν_1 or $\nu_0 - \nu_1$, the inverting modulator may become inoperative. The same applies to the non-inverting modulator.

Since an infinitesimally narrow filter bandwidth is not realizable physically, we conclude that the foregoing inverting and non-inverting modulators can be realized physically only under an additional limitation, not mentioned in reference 11. This limitation presupposes that the nonlinear reactive element or oscillations are sufficiently small, such that the intensity of the higher combination frequencies that enter in the pass band of the reactive filters is negligibly small.

It was indicated at the end of Sec. 1 that the impossibility of converting ac into dc (or vice versa) by means of a reactive nonlinearity agrees with the general power equations of Manly and Rowe.

Actually, let us assume that one of the combination frequencies, generated by the reactive nonlinearity, vanishes.

$$m_1\nu_0 + n_1\nu_1 = 0.$$

The corresponding power must also vanish

$$P_{m_1, n_1} = 0,$$

for in the opposite case the term

$$\frac{P_{m_1, n_1}}{m_1\nu_0 + n_1\nu_1}$$

would become infinite, a physical impossibility.

To conclude this section let us also dwell briefly on the influence of hysteresis.[11] Hysteresis introduces an irreversibility in the relation between the charge and voltage of a nonlinear capacitor. This makes the integrals in the right halves of (2.11′) and (2.12′) no longer equal to zero. In the general case, the power equations become exceedingly more complicated. But there is one particular case when the equations remain simple, even with hysteresis. This is when the carrier is at a high level and the signal at low level. It should be noted that a high carrier level can occur when little power is drawn at the carrier frequency, i.e., at low $P_{1,0}$. This

level is set by the voltage applied by the carrier generator, and $P_{1,0}$ depends on the control signal.

Actually, in the presence of hysteresis, the variation charge vs. voltage curve is complicated and in general not closed (if ν_0 and ν_1 are not commensurate). But if the intensity of the carrier is high, then the hysteresis loop will be determined essentially by the carrier, and the other oscillations will merely cause slight variations, barely affecting the energy associated with the loop. It is permissible to consider the loop to be approximately double-valued and to carry out the integration in the right halves of (2.11′) and (2.12′).

We choose the lower part of the hysteresis curve for increasing charge and the upper one for decreasing charge (Fig. 14). Then the right half of the (2.11′) becomes

$$h = \oint \varphi(q)\, dq,$$

i.e., the area inside the hysteresis loop or the energy lost to hysteresis per cycle of carrier. The power H lost to hysteresis will be correspondingly

$$H = h\nu_0. \tag{2.24}$$

Thus, Eq. (2.11′), for hysteresis in the form of a double-valued loop, yields the power equation

$$\sum_{m=0}^{+\infty}\sum_{n=-\infty}^{+\infty} \frac{mP_{m,n}}{m\nu_0 + n\nu_1} = \frac{H}{\nu_0}. \tag{2.16′}$$

In the right half of (2.12′) the function $\varphi(q)$ is integrated along the curve connected with the variation of y, i.e., with the frequency ν_1 of the signal. Under the simplifications made here, the function will be periodic, and consequently, its integral will still vanish, as in the absence of hysteresis. Equation (2.17) therefore remains unchanged even if hysteresis is taken into account.

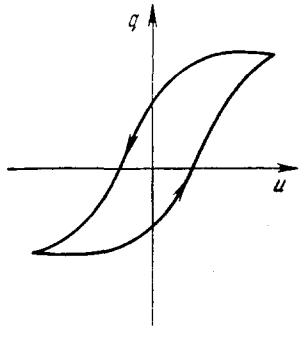

FIG. 14. Allowance for hysteresis in the power equations.

It is easy to see that H/ν_0 can be moved to the left of (2.16′) and combined with the component $P_{1,0}$ into a term of the form

$$\frac{P_{1,0} - H}{\nu_0}.$$

Consequently, the change produced by allowance for hysteresis reduces to substracting the power loss due to hysteresis from the power drawn from the generator. We repeat: we have considered the effect of hysteresis under greatly simplifying assumptions.

3. ANALYSIS OF THE REACTIVE MODULATOR BY THE SMALL-SIGNAL METHOD

The general power relations considered in Sec. 2 do not yield detailed information on devices with nonlinear reactances. For a more detailed analysis it is necessary to make the problem more specific. Calculation of nonlinear circuits without simplifying assumptions is complicated. In the case of a reactive modulator that does not become unstable, the problem can be simplified by linearization. Reactive modulators were analyzed by Rowe,[13] Bloom and Chang,[14] Heffner and Wide,[15] and by Leenov,[16] who used small-signal linearization. We shall employ a similar analysis with certain modifications, which are of no principal significance, but which help to explain better, from our point of view, the operation of a two-loop reactive modulator.

Assume that the charge q and the voltage u are related by the singled-valued function

$$q = f(u). \tag{3.1}$$

Let furthermore only a voltage u_0, from a local carrier generator of frequency ν_0, be applied to the capacitor in the absence of a signal. In this case the alternating charge q_0 will be, in accordance with (3.1),

$$q_0 = f(u_0).$$

The spectrum of the oscillations of alternating charge q_0, like those of the voltage u_0, contain in the absence of a signal the fundamental frequency ν_0 and its harmonics. We assume, further, that the signal voltage δu across the nonlinear reactance is small compared with u_0, and the variation of the charge is likewise small. The charge variation can then be related to the voltage variation by a linear equation (using the concept of differential capacitance), as has been done at the start of Sec. 1

$$\delta q = C_i(u_0)\,\delta u, \tag{3.2}$$

where $C_i(u_0) = df(u_0)/du$ is a capacitance, independent of the magnitude of the signal, but variable in time and periodic in the fundamental frequency ν_0. The time variation of C_i is determined by the character of the nonlinearity and by the amplitude and waveform of the oscillations from the local generator. The remaining calcula-

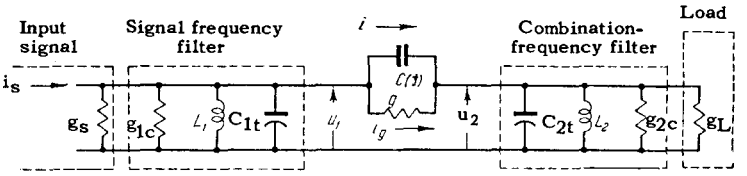

FIG. 15. Diagram of two-loop reactive modulator.

tions will be carried out in the linear treatment for a system with a variable, pulsating capacitance.

If we are not interested in calculating the nonlinear distortion of the reactive modulator, we can simplify the problem immediately by dispensing with the local generator. We assume that the local generator modulates the capacitance C in a very simple manner at a frequency $\omega_0 = 2\pi\nu_0$, without harmonics:

$$C(t) = C_0(1 + m\cos\omega_0 t). \tag{3.3}$$

Let us consider now the two-loop reactive modulator shown in Fig. 15. The signal frequency ν_S will be considered to differ greatly from the carrier frequency ν_0. The first resonant circuit with conductance g_{1C}, inductance L_1, and trimming capacitor C_{1t} serves to suppress all frequencies with the exception of ν_S, while the second resonant circuit, g_{2C}, L_2 and C_{2t} leaves only one of the combination frequencies, $\nu_0 + \nu_S$ or $\nu_0 - \nu_S$. The loops are coupled by the nonlinear capacitance C(t) which pulsates as in (3.3), and the losses are represented by the conductance g. We assume that both loops have sufficient Q to make them practically equivalent to a short circuit at all combination frequencies except the resonant ones.

Were the capacitance C of Fig. 15 constant, the analysis of the circuit would reduce to the solution of a system of two linear second-order equations with constant coefficients. The general solution of this system with specified initial conditions would determine the entire transient process, while the particular solution in response to a sinusoidal signal would determine only the steady-state harmonics. The steady state process could be evaluated very simply by the impedance method. But since the capacitance C pulsates, analysis of the circuit requires a solution of equations with variable coefficients; if the modulation is as in Eq. (3.3), a Mathieu type equation must be solved. The general solution again gives the complete picture, including the transients in the loops, while the particular solution in response to a sinusoidal signal gives only the steady-state process. Here, too, the steady state can be determined by the impedance method, with slight modifications. Since the system remains linear, the principle of superposition can still be employed.

The complete solution of the differential equations with variable coefficients for the circuit of Fig. 15 involves no special difficulties. In particular, a system of two linear equations with variable coefficients can be reduced by operational calculus* to a single equation of the same order, but of higher degree. In the present article however, we do not consider the transients and confine ourselves only to the steady state, which is evaluated much more simply.

Since the principle of superposition holds in our system we can solve the problem by the ordinary impedance method by merely finding the current in the pulsating capacitance upon application of a sinusoidal voltage

$$u(t) = U\cos(\omega t + \varphi) \tag{3.4}$$

with arbitrary frequency ω and phase φ.

To use the complex-amplitude method in the calculations, we replace (3.4) by the complex function

$$\dot{u} = \dot{U}e^{j\omega t}, \tag{3.5}$$

where $\dot{U} = Ue^{j\varphi}$, and (3.3) is transformed identically to

$$C_0(1 + m\cos\omega_0 t) \equiv C_0 + \frac{1}{2}mC_0e^{j\omega_0 t} + \frac{1}{2}mC_0e^{-j\omega_0 t}. \tag{3.6}$$

The initial sinusoidal voltage (3.4) corresponds to the real part of (3.5)

$$u(t) = U\cos(\omega t + \varphi) = \mathrm{Re}\,\dot{u}. \tag{3.7}$$

The charge q on a linear capacitance C(t) is

$$q = C\cdot u$$

and consequently, the current i(t) through the capacitance will be

$$i = \frac{dq}{dt} = \frac{d}{dt}(C\cdot u). \tag{3.8}$$

If we insert the complex functions (3.5) and (3.6) into the right half of (3.8), we obtain on the left hand the complex function $\dot{i}$

$$\dot{i} = j\omega C_0\dot{U}e^{j\omega t} + j(\omega + \omega_0)\frac{1}{2}mC_0\dot{U}e^{j(\omega+\omega_0)t} + j(\omega - \omega_0)\frac{1}{2}mC_0\dot{U}e^{j(\omega-\omega_0)t}. \tag{3.9}$$

*See, for example, Van der Pol and Bremmer, Operational Calculus, Cambridge University Press, 1950, Chapter X (Russian translation, M., 1952).

The real part of the complex function $\dot{i}$ yields for the current i(t)

$$i(t) = \mathrm{Re}\,\dot{i} = -\omega C_0 U \sin(\omega t + \varphi) - (\omega_0 + \omega)\frac{1}{2} mC_0 U \sin[(\omega_0 + \omega)t + \varphi] - (\omega_0 - \omega)\frac{1}{2} mC_0 U \sin[(\omega_0 - \omega)t - \varphi], \quad (3.10)$$

This can be readily verified by calculating i(t) directly from (3.3) and (3.4). We conclude hence that the difference between a capacitance C(t), pulsating sinusoidally with frequency ω_0 and depth of modulation m, and a fixed capacitance C_0 is that a sinusoidal voltage of frequency ω produces, in addition to a current of fundamental frequency ω, also sinusoidal currents at combination frequencies $\omega + \omega_0$ and $\omega - \omega_0$. All three currents can be calculated by the complex-impedance (or complex admittance) method, assuming the admittances of the capacitance to be, for each component of the triplet,

$$j\omega C_0, \quad j(\omega + \omega_0)\frac{1}{2} mC_0 \text{ and } j(\omega - \omega_0)\frac{1}{2} mC_0, \quad (3.11)$$

and assuming the voltage to be represented by

$$\dot{U}e^{j\omega t}, \quad \dot{U}e^{j(\omega+\omega_0)t} \text{ and } \dot{U}e^{j(\omega-\omega_0)t}. \quad (3.12)$$

The appearance of the combination frequencies in a pulsating capacitance is an indication of its modulating properties.

From an examination of the effect of a pulsating capacitance it is clear only its variable part $mC_0 \times \cos \omega_0 t$ produces the combination frequencies, while the fixed C_0 merely combines with the trimming capacitances C_{1t} and C_{2t} (Fig. 15).

If we denote

$$\left.\begin{aligned} C_{1t} + C_0 &= C_1, & C_{2t} + C_0 &= C_2; \\ g_s + g_{1c} + g &= g_1, & g_{2c} + g_L + g' &= g_2 \end{aligned}\right\} \quad (3.13)$$

and

$$mC_0 = \Delta C, \quad (3.14)$$

then the circuit of Fig. 15 can be replaced by that of Fig. 16, and the coupling current will contain only two amplitudes at the combination frequencies. The reason that the fixed portions C_0 of the coupling capacitor and the conductance g are so readily calculated is that the loops are fully uncoupled in frequency: the second loop is a short circuit at the frequency ν_S, and the first one is a short circuit at the combination frequency to which the second loop is tuned, i.e., $\nu_0 + \nu_S$ or $\nu_0 - \nu_S$. Since the coupling-capacitor losses depend on the frequency, they are represented by g in the first loop and g' in the second loop.

1. Non-Inverting Modulator with Summary Combination Frequency $\omega_2 = \omega_0 + \omega_1$

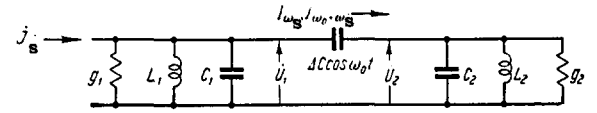

FIG. 16. Reduced equivalent circuit of two-loop reactive modulator.

The signal

$$i_s = J_s \cos(\omega_s t + \varphi_s) = \mathrm{Re}[\dot{J}_s e^{j\omega_s t}] \quad (3.15)$$

is fed from a current generator with internal conductance g_S.

We denote the admittance of the first and second loops respectively by

$$\left.\begin{aligned} \dot{Y}_1(\omega) &= g_1 + j\left(\omega C_1 - \frac{1}{\omega L_1}\right) = g_1 + jX_1, \\ \dot{Y}_2(\omega) &= g_2 + j\left(\omega C_2 - \frac{1}{\omega L_2}\right) = g_2 + jX_2, \end{aligned}\right\} \quad (3.16)$$

and their resonant frequencies by

$$\omega_1 = 2\pi\nu_1 = \frac{1}{\sqrt{L_1 C_1}}, \qquad \omega_2 = 2\pi\nu_2 = \frac{1}{\sqrt{L_2 C_2}}. \quad (3.17)$$

Let the signal frequency $\omega_S = 2\pi\nu_S$ be close to ω_1. Then the combination frequency $\omega_0 + \omega_S$ will be close to $\omega_2 = \omega_0 + \omega_1$. The first loop will separate the sinusoidal voltage at the signal frequency

$$u_1(t) = \mathrm{Re}[\dot{U}_1 e^{j\omega_s t}], \quad (3.18)$$

and the second loop the voltage at the summary combination frequency $\omega_0 + \omega_S$

$$u_2(t) = \mathrm{Re}[\dot{U}_2 e^{j(\omega_0+\omega_s)t}]. \quad (3.19)$$

The current $\Delta i(t)$ through the pulsating capacitance $\Delta C \cos \omega_0 t$ can be readily found in accordance with the rule developed above. Its value is

$$\Delta i(t) = \mathrm{Re}\left[-j\omega_s \frac{1}{2}\Delta C \dot{U}_2 e^{j\omega_s t} + j(\omega_0 + \omega_s)\frac{1}{2}\Delta C \dot{U}_1 e^{j(\omega_0+\omega_s)t}\right]. \quad (3.20)$$

We shall henceforth omit the symbol Re, agreeing, as is usually done in calculations by the impedance method, to take only the real part of the final complex expression.

Knowing the amplitudes of the coupling current

$$\dot{I}_{\omega_s} = -j\omega_s \frac{1}{2}\Delta C \dot{U}_2, \quad \dot{I}_{\omega_0+\omega_s} = j(\omega_0 + \omega_s)\dot{U}_1, \quad (3.20')$$

we can readily find the amplitudes of all the currents and voltages in the circuit of Fig. 16, expressed in terms of the amplitude of the signal current J_S. The voltages in the first and second loop are of the form

$$\left.\begin{aligned} \dot{U}_1 &= \frac{\dot{Y}_2(\omega_0+\omega_s)}{\dot{Y}_1(\omega_s)\dot{Y}_2(\omega_0+\omega_s) + \left(\frac{1}{2}\Delta C\right)^2 \omega_s(\omega_0+\omega_s)} \dot{J}_s, \\ \dot{U}_2 &= \frac{j(\omega_0+\omega_s)\frac{1}{2}\Delta C}{\dot{Y}_1(\omega_s)\dot{Y}_2(\omega_0+\omega_s) + \left(\frac{1}{2}\Delta C\right)^2 \omega_s(\omega_0+\omega_s)} \dot{J}_s. \end{aligned}\right\} \quad (3.21)$$

Expressions (3.21) are analogous to the formulas for the voltages produced in ordinary coupled circuits by an applied sinusoidal voltage. The difference lies in that the loop admittances $\dot{Y}_1(\omega_S)$ and $\dot{Y}_2(\omega_0 + \omega_S)$ are functions of different frequencies; in analogy with ordinary coupled circuits, we introduce the coupling admittance

$$X_{coup} = \frac{1}{2}\Delta C \sqrt{\omega_S(\omega_0 + \omega_S)} \tag{3.22}$$

and denote

$$\dot{\gamma}_{2+} = \frac{X_{coup}}{\dot{Y}_2(\omega_0+\omega_S)} = \frac{X_{coup}}{Y_2(\omega_0+\omega_S)} e^{-j\varphi_2} = \gamma_{2+} e^{-j\varphi_2}, \tag{3.23}$$

where $\varphi_2 = \tan^{-1}(X_2/g_2)$. We then obtain for the voltage in the first loop the following expression

$$\dot{U}_1 = \frac{1}{\dot{Y}_1(\omega_S) + \gamma_{2+}^2 \dot{Y}_2^*(\omega_0+\omega_S)} \dot{J}_S, \tag{3.24}$$

and for the ratios of U_2 to U_1 (of different frequencies!) we have

$$\frac{\dot{U}_2}{\dot{U}_1} = j\sqrt{\frac{\omega_0+\omega_S}{\omega_S}}\,\dot{\gamma}_{2+}. \tag{3.25}$$

Relation (3.24) shows that the impedance introduced into the first (input) loop is determined in the same manner as the impedance introduced in ordinary coupled networks, and that the equivalent admittance of the first loop has the form

$$\dot{Y}_{1\,eq} = \{g_1 + g_+\} + j(X_1 - \gamma_{2+}^2 X_2), \tag{3.26}$$

where $g_+ = \gamma_{2+}^2 g_2$ is the active conductance introduced into the first loop. Since γ_{2+}^2 is a positive quantity, the frequency conversion is accompanied by the insertion of positive resistance, i.e., by flow of energy from the signal source to the modulator. Consequently, the non-inverting modulator is always stable.

Let us find the power P_{ω_S} fed from the signal source to the modulator (disregarding losses in the conductance g_1). In accordance with (3.20), (3.23), (3.24), (3.25), and (3.26) we have

$$P_{\omega_S} = I_{\omega_S} \cdot U_1 \cos(\dot{I}_{\omega_S}\dot{U}_1) = \frac{g_+}{|\dot{Y}_{1\,eq}|^2}|\dot{J}_S|^2. \tag{3.27}$$

The power $P_{\omega_0+\omega_S}$ fed to g_2 from the reactive converter is considered negative, as agreed upon in Sec. 2. Its value is

$$-P_{\omega_0+\omega_S} = I_{\omega_0+\omega_S} U_2 \cos\varphi_2 = \frac{\omega_0+\omega_S}{\omega_S}\frac{g_+}{|\dot{Y}_{1\,eq}|^2}|\dot{J}_S|^2. \tag{3.28}$$

The power gain G_+ is

$$G_+ = \frac{-P_{\omega_0+\omega_S}}{P_{\omega_S}} = \frac{\omega_0+\omega_S}{\omega_S}, \tag{3.29}$$

in exact agreement with (2.20).

However, the power fed to g_2 flows only partially to the load g_{2L}; the corresponding fraction is g_{2L}/g_2. In exactly the same manner, part of the power from the signal generator is consumed nonproductively in g_{1C} and g. Considering furthermore that the maximum power that the signal generator can deliver to the modulator is

$$(P_{\omega_S})_{max} = \frac{1}{4}\frac{|\dot{J}_S|^2}{g_S} \tag{3.30}$$

and under perfect matching at that, we can determine the actual power gain K_+ of the non-inverting modulator, with allowance for losses and mismatch

$$K_+ = \frac{-P_L}{(P_{\omega_S})_{max}} = \frac{\omega_0+\omega_S}{\omega_S}\frac{4g_S\cdot g_+}{|\dot{Y}_{1\,eq}|^2}\frac{g_{2L}}{g_2} = G_+\frac{4g_S g_+}{|\dot{Y}_{1\,eq}|^2}\frac{g_{2L}}{g_2}. \tag{3.31}$$

Using (3.31) we can investigate the dependence of the power gain K_+ on the frequency and on the parameters of the modulator circuit.

Let us examine K_+ under small detuning, i.e., let us assume that

$$\Delta\omega = \omega_S - \omega_1 \tag{3.32}$$

satisfies the inequalities

$$\left|\frac{\Delta\omega}{\omega_1}\right| \ll 1, \quad \left|\frac{\Delta\omega}{\omega_2}\right| \ll 1. \tag{3.33}$$

In this case we can introduce the approximate relations

$$\begin{aligned}\dot{Y}_1(\omega_S) &\cong g_1(1 + jQ_1\cdot 2\xi_1),\\ \dot{Y}_2(\omega_0+\omega_S) &\cong g_2(1 + jQ_2\cdot 2\xi_2),\end{aligned} \tag{3.34}$$

where

$$Q_1 = \frac{\omega_1 C_1}{g_1}, \quad Q_2 = \frac{\omega_2 C_2}{g_2};$$
$$\xi_1 = \frac{\Delta\omega}{\omega_1}, \quad \xi_2 = \frac{\Delta\omega}{\omega_2}.$$

The approximate value of γ_{2+}^2 is

$$\gamma_{2+}^2 \cong \gamma_{20}^2\frac{(1+\xi_1)(1+\xi_2)}{1+(Q_2\cdot 2\xi_2)^2} \cong \gamma_{20}^2\frac{1}{1+(Q_2\cdot 2\xi_2)^2}, \tag{3.35}$$

where

$$\gamma_{20}^2 = \frac{\left(\frac{1}{2}\Delta C\right)^2\omega_1\omega_2}{g_2^2}$$

The resistance introduced into the first loop is given by the approximate relation

$$g_+ = \gamma_{2+}^2 g_2 \cong g_0\frac{1}{1+(Q_2\cdot 2\xi_2)^2}, \tag{3.36}$$

where

$$g_0 = \gamma_{20}^2 g_2.$$

Using (3.34) — (3.36) we can represent K_+, for small detuning, by

$$K_+ = G_+\frac{4g_S g_0\frac{g_{2L}}{g_2}}{\left|g_1(1+jQ_1\cdot 2\xi_1) + g\frac{1-jQ_2\cdot 2\xi_2}{1+(Q_2\cdot 2\xi_2)^2}\right|^2}. \tag{3.37}$$

If we neglect the losses in g_{ic}, g, g_{2c}, and g' we obtain in (3.37) $g_S = g_1$ and $g_{2L} = g_2$. In coupled networks at multiple resonance, the imaginary part of $\dot{Y}_{1\,eq} \cong g_1 + g_+ + j(g_1Q_1 \cdot 2\xi_1 - g_+Q_2 \cdot 2\xi_2)$ vanishes, i.e.,

$$(g_1Q_1 \cdot 2\xi_1 - g_+Q_2 \cdot 2\xi_2) = 0. \tag{3.38}$$

In complex resonance, furthermore, the coupling between the networks should be optimal,

$$X_{coup} = (X_{coup})_{opt} = Y_2 \sqrt{\frac{g_1}{g_2}} \approx [1 + (Q_2 \cdot 2\xi_2)^2] \sqrt{g_1 g_2}, \tag{3.39}$$

i.e.,

$$g_0 = g_1. \tag{3.40}$$

Inserting (3.38) and (3.40) into (3.37) we get

$$(K_+)_{max} = G_+,$$

i.e., in a reactive non-inverting modulator, as in an ordinary coupled network, maximum power is delivered to the second loop at optimum coupling and complex resonance. In this case the input and the output are fully matched. But relation (3.38) can be realized in an infinite number of manners, at various values of ξ_1 and ξ_2 in (3.38), and it follows hence that the matching of the modulator loops, producing a maximum gain $K_+ = G_+$, leaves a degree of freedom for the variation of the reactive input and output elements. This degree of freedom can be used to select the optimum bandwidth of the modulator. Let us assume that

$$g_1 = g_2 = g_0, \quad \gamma_{20} = 1. \tag{3.41}$$

Then the complex resonance becomes complete resonance and

$$Q_1\xi_1 = \frac{C_1}{g_0}\Delta\omega, \quad Q_2\xi_2 = \frac{C_2}{g_0}\Delta\omega.$$

If we consider that $C_1 = C_{1t} + C_0 \cong C_2 = C_{2t} + C_0$, we can introduce a generalized detuning x, equal to

$$x = 2\sqrt{\frac{C_1C_2}{g_1g_2}}\Delta\omega \approx Q_1 \cdot 2\xi_1, \quad x \approx Q_2 \cdot 2\xi_2. \tag{3.42}$$

Inserting (3.41) and (3.42) in (3.37) we get

$$K_+ = G_+ \frac{4\frac{1}{1+x^2}}{\left|1 + jx + \frac{1}{1+jx}\right|^2} = G_+ \frac{1}{1 + \left(\frac{x}{\sqrt{2}}\right)^2}. \tag{3.43}$$

If we specify a 3-db reduction in gain, we find the corresponding bandwidth, by putting $K_+ = \frac{1}{2}$ in (3.43)

$$x = \bar{x} = \pm\sqrt{2}, \tag{3.44}$$

i.e.,

$$\frac{2\overline{\Delta\omega}}{\omega_1} = \sqrt{2}\frac{1}{Q_1}, \quad \frac{2\overline{\Delta\omega}}{\omega_2} = \sqrt{2}\frac{1}{Q_2}. \tag{3.45}$$

We see that the bandwidth of a non-inverting modulator is $\sqrt{2}$ times wider than that of the corresponding single-loop network. In a system of two identical optimally-coupled networks the bandwidth is also $\sqrt{2}$ times wider than that of each loop; the analogy becomes complete for the relative bandwidth at the geometric mean frequency

$$\frac{2\overline{\Delta\omega}}{\sqrt{\omega_1\omega_2}} = \sqrt{2}\frac{1}{\sqrt{Q_1Q_2}}. \tag{3.45'}$$

Under total resonance the coupling coefficient k of the loops of a non-inverting modulator equals the reciprocal of the geometric mean of the Q's of the two loops

$$k = \frac{\frac{1}{2}\Delta C\sqrt{\omega_1\omega_2}}{\sqrt{\omega_1C_1 \cdot \omega_2C_2}} = \frac{1}{\sqrt{Q_1Q_2}}. \tag{3.46}$$

For the absolute value of the band with $2\overline{\Delta\omega}$ we obtain the following expression

$$2\overline{\Delta\omega} = \frac{\frac{1}{2}\Delta C}{\sqrt{C_1C_2}}\sqrt{2\omega_1\omega_2} = k\sqrt{2\omega_1\omega_2}. \tag{3.47}$$

As is known, in a system of two coupled identical loops the maximum width at the 3-db level is obtained at a coupling greater than optimal, namely at

$$k = (1 + \sqrt{2})\frac{1}{Q}.$$

Here the resonance curve acquires two humps, the reduction of the amplitude at the center of the band reaches 3 db, and the relative bandwidth is

$$\frac{2\overline{\Delta\omega}}{\omega_0} = 2\sqrt{1 + \sqrt{2}}\,\frac{1}{Q} \cong 3{,}1\,\frac{1}{Q},$$

i.e., approximately three times greater than the bandwidth of the single loop. The same situation occurs also for the bandwidth of the reactive non-inverting modulator considered here. Putting

$$k = \frac{\frac{1}{2}\Delta C}{\sqrt{C_1C_2}} = (1 + \sqrt{2})\frac{1}{\sqrt{Q_1Q_2}},$$

we obtain for the bandwidth

$$\frac{2\overline{\Delta\omega}}{\sqrt{\omega_1\omega_2}} = 2\sqrt{1 + \sqrt{2}}\,\frac{1}{\sqrt{Q_1Q_2}}.$$

Thus, we arrive at the conclusion that the frequency characteristic of the investigated non-inverting modulator is analogous to the frequency characteristic of two identical coupled networks.

Let us examine a numerical example. Assume a signal frequency ν_S = 100 Mcs (λ_S = 3 m), a summary frequency $\nu_0 + \nu_S$ = 20,000 Mcs (λ_+ = 1.5 cm), and a carrier frequency ν_0 = 19,900 Mcs.

The gain at the center of the band will be

$$G_+ = 200, \quad 10 \log G_+ = +23 \text{ db}.$$

The bandwidth is determined by the relation

$$2\overline{\Delta\nu} = 2000\, k \text{ Mcs}; \quad \left(\frac{2\overline{\Delta\nu}}{100}\right)_{\text{Mcs}} = 10\frac{\Delta C}{\sqrt{C_1C_2}}.$$

We see that even at a very small depth of modulation, when $\Delta C/\sqrt{C_1C_2}$ amounts to merely 1%, the bandwidth may reach 10 Mcs.

It must be borne in mind, however, that the calculation results may be substantially modified by the losses g and g′ of the coupling capacitor. Let us find an expression for K_+ at exact tuning ($\xi = 0$) with allowance for g and g′ (if the two loops have high Q, g_{1C} and g_{2C} can be disregarded). From (3.37) we obtain

$$(K_+)_{\xi_{1,2}=0} = \frac{\omega_2}{\omega_1}\frac{4g_S \cdot g_{2L}\left(\frac{1}{2}\Delta C\right)^2 \omega_1\omega_2}{\left[(g_S+g)(g_{2L}+g') + \left(\frac{1}{2}\Delta C\right)^2 \omega_1\omega_2\right]^2}.$$

Assuming g, g′, and ΔC to be specified by the power pumping device, we can determine the maximum value of K_+ by selecting g_S and g_{2L}. Calculation yields

$$(K_+)'_{\max} = \frac{\omega_2}{\omega_1}\frac{1}{(\tan\delta_p + \sqrt{1+\tan^2\delta_p})^2}. \tag{3.48}$$

In Eq. (3.48),

$$\tan\delta_p = \sqrt{\frac{gg'}{\frac{1}{2}\Delta C\omega_1 \cdot \frac{1}{2}\Delta C\omega_2}} \tag{3.49}$$

can be called the parametric tangent of the loss angle, which characterizes the energy losses in a coupling capacitor with pulsating capacitance. When $\tan\delta_p \gg 1$ we have

$$(K_+)'_{\max} \cong \frac{\omega_2}{\omega_1 \cdot 4\tan^2\delta_p}$$

and $(K_+)'_{\max} \leq 1$, i.e., amplification is impossible if $\tan^2\delta_p \geq 0.25\,(\omega_2/\omega_1)$.

2. Inverting Modulator with Differential Combination Frequency $\omega_2 = \omega_0 - \omega_1$

The voltage drops across the resonant circuits of the modulator are

$$\dot{u}_1(t) = \dot{U}_1 e^{j\omega_S t}, \quad \dot{u}_2(t) = \dot{U}_2 e^{j(\omega_0-\omega_S)t}$$

The coupling current through the pulsating capacitance is

$$\Delta i(t) = j\omega_S\frac{1}{2}\Delta C\dot{U}_2 e^{-j\omega_S t} - j(\omega_0-\omega_S)\frac{1}{2}\Delta C\dot{U}_1 e^{-j(\omega_0-\omega_S)t} + \ldots$$

The complex coupling-current amplitudes of interest to us are, respectively

$$\dot{I}'_{\omega_S} = -j\omega_S\frac{1}{2}\Delta C\dot{U}_2^*; \quad \dot{I}_{\omega_0-\omega_S} = j(\omega_0-\omega_S)\frac{1}{2}\Delta C\dot{U}_1^*. \tag{3.50}$$

From calculations analogous to those made for the non-inverting modulator we get

$$\dot{U}_1 = \frac{1}{\dot{Y}_{1\,\text{eq}}}\dot{J}_c, \tag{3.51}$$

$$\frac{\dot{U}_2}{\dot{U}_1} = -j\frac{X_{\text{coup}}}{\dot{Y}_2^*(\omega_0-\omega_S)} = -j\dot{\gamma}_{2-}^* \sqrt{\frac{\omega_0-\omega_S}{\omega_S}}, \tag{3.52}$$

$$\left.\begin{aligned}
&\dot{Y}_1(\omega_S) = g_1 + j\left(\omega_S C_1 - \frac{1}{\omega_S L_1}\right),\\
&\dot{Y}_2(\omega_0-\omega_S) = g_2 + j\left[(\omega_0-\omega_S)C_2 - \frac{1}{(\omega_0-\omega_S)L_2}\right],\\
&\dot{\gamma}_{2-}^* = \frac{X_{\text{coup}}}{\dot{Y}_2^*} = \gamma_{20}e^{j\varphi_2}, \quad \gamma_{20} = \frac{X_{\text{coup}}}{\dot{Y}_2}; \quad \varphi_2 = \tan^{-1}\frac{\operatorname{Re}\dot{Y}_2}{\operatorname{Im}\dot{Y}_2},\\
&\dot{Y}_{1\,\text{eq}} = \dot{Y}_1(\omega_S) - |\dot{\gamma}_{2-}^*|^2\dot{Y}_2(\omega_0-\omega_S)\\
&\quad = g_1 - g_- + j\operatorname{Im}[\dot{Y}_1(\omega_S) - \dot{\gamma}_{2-}^2\dot{Y}_2(\omega_0-\omega_S)],\\
&g_- = \gamma_{2-}^2 g_2.
\end{aligned}\right\} \tag{3.53}$$

The gain G_- is found to be

$$G_- = -\frac{\omega_0-\omega_S}{\omega_S}, \tag{3.54}$$

in exact accordance with (2.23). The inverting modulator is actually found to be potentially unstable, for, as follows from (3.53), the conductance g_- introduced in the first loop enters into $\dot{Y}_{eq}$ with a negative sign. The system loses stability when $g_1 - g_- \leq 0$. Introducing K_-, the gain of the entire inverting modulator, analogous to K_+ of the non-inverting modulator [see (3.31)], we obtain

$$K_- = G_-\frac{-4g_S g_-}{|\dot{Y}_{1\,\text{eq}}|^2}\frac{g_{2L}}{g_2}, \tag{3.55}$$

where $\dot{Y}_{1\,eq}$ and g_- are determined from (3.53). Let us analyze K_- at small detunings and under all the other simplifications introduced in the analysis of the non-inverting modulator. In this case it is necessary to replace everywhere the summary frequency $\omega_0 + \omega_S$ of the non-inverting modulator by the differential frequency $\omega_0 - \omega_S$ of the inverting modulator. We obtain

$$\left.\begin{aligned}
&\dot{Y}_1 \approx g_1(1 + jQ_1\cdot 2\xi_1), \quad Q_1 = \frac{\omega_1 C_1}{g_1}, \quad \xi_1 = \frac{\Delta\omega}{\omega_1} = \frac{\omega_2-\omega_1}{\omega_1};\\
&\dot{Y}_2 \approx g_2(1 - jQ_2\cdot 2\xi_2), \quad Q = \frac{\omega_2 C_2}{g_2},\\
&\xi_2 = \frac{\Delta\omega}{\omega_2} = \frac{\omega_2-(\omega_0-\omega_S)}{\omega_2} = \frac{\omega_S-\omega_1}{\omega_2};\\
&|\xi_1| \ll 1, \quad |\xi_2| \ll 1; \quad g_1 = g_2 = g; \quad C_1 \approx C_2;\\
&x = 2\sqrt{\frac{C_1C_2}{g_1g_2}}\,\Delta\omega \approx Q_1\cdot 2\xi_1, \quad x \approx Q_2\cdot 2\xi_2;\\
&\gamma_{2-}^2 = \gamma_{20}^2\frac{1}{1+x^2}, \quad \gamma_{20}^2 = \frac{\left(\frac{1}{2}\Delta C\right)^2\omega_1\omega_2}{g_2^2};\\
&\frac{\dot{Y}_{1\,\text{eq}}}{g_1} = 1 + jx - \frac{\gamma_{20}^2}{1+jx}; \quad g_- = g_0\frac{1}{1+x^2}, \quad g_0 = \gamma_{20}^2 g_2 = \gamma_{20}^2 g_1.
\end{aligned}\right\} \tag{3.56}$$

Inserting into (3.55) the values of $\dot{Y}_{1\,eq}$ and g_- from (3.56), we obtain the dependence of the gain K_- on the detuning x and on the quantity γ_{20}^2, which characterizes the parametric coupling of the loops

$$K_- = G_- \frac{-4\frac{\gamma_{20}^2}{1+x^2}\frac{g_s g_{2L}}{g_0^2}}{\left|1+jx-\frac{\gamma_{20}^2}{1+jx}\right|^2} = \frac{\omega_0-\omega_s}{\omega_s}\frac{4\gamma_{20}^2\frac{g_s g_{2L}}{g_0^2}}{(1-\gamma_{20}^2)^2}\frac{1}{1+2\frac{1+\gamma_{20}^2}{(1-\gamma_{20}^2)^2}x^2+\frac{1}{(1-\gamma_{20}^2)^2}x}. \quad (3.57)$$

At zero detuning (x = 0) the gain K_- becomes

$$K_-\Big|_{x=0} = \frac{\omega_2}{\omega_1}\frac{\frac{g_s g_{2L}}{g_0^2}}{(1-\gamma_{20}^2)^2}. \quad (3.57')$$

Since the resistance introduced into the first loop is negative, the input can no longer be matched to the output, as in the non-inverting modulator; K_- can be made as large as desired by reducing the losses in the input circuit.

When

$$\gamma_{20}^2 \geqslant 1$$

the inverting modulator becomes unstable. But even when γ_{20}^2 is less than but sufficiently close to 1, the instability in the inverting modulator increases rapidly. Instability of a radio device is frequently characterized by the sensitivity S of the device to small changes of some particular parameter, defined as the relative change in the gain divided by the relative change in the parameter causing the change. It is clear that for good stability a device should have a low sensitivity S. At the center of the band, when the input and the output are matched, the gain ($K_+ = G_+$) of the non-inverting modulator is independent of either the active conductance $g_1 = g_2 = g_0$ or of the amplitude of the capacitance pulsations ΔC. Therefore

$$S_{+g} = \frac{\partial K_+}{\partial g_0}\frac{g_0}{K_+} = 0; \qquad S_{+\Delta C} = \frac{\partial K_+}{\partial \Delta C}\frac{\Delta C}{K_+} = 0. \quad (3.58)$$

The sensitivity of an inverting modulator, S_-, does not vanish. In the center of the band, depending on the conductance $g_1 = g_2$ in the amplitude of the capacitance pulsations ΔC, it has the form

$$S_{-g} = \frac{\partial K_-}{\partial g_1}\frac{g_1}{K_-} = -2\frac{1+\gamma_{20}^2}{1-\gamma_{20}^2}; \quad S_{-\Delta C} = \frac{\partial K_-}{\partial \Delta C}\frac{\Delta C}{K_-} = -S_{-g}. \quad (3.59)$$

As $\gamma_{20}^2 \to 1$, the instability of the inverting modulator is characterized by a sensitivity that approaches infinity.

The bandwidth of the inverting modulator at the 3-db level is determined by setting the last factor of (3.57) equal to ½

$$\frac{1}{2} = \frac{1}{1+2\frac{1+\gamma_{20}^2}{(1-\gamma_{20}^2)^2}x^2+\frac{1}{(1-\gamma_{20}^2)^2}x^4}. \quad (3.60)$$

Let us consider the bandwidth as γ_{20}^2 approaches unity. Solution of (3.60) yields in this case

$$x = \pm\frac{1}{2}(1-\gamma_{20}^2)$$

or

$$2\overline{\Delta\omega} = \frac{1}{2}\frac{\Delta C}{\sqrt{C_1 C_2}}\sqrt{\omega_1\omega_2}(1-\gamma_{20}^2) = k\sqrt{\omega_1\omega_2}(1-\gamma_{20}^2)$$

for $(1-\gamma_{20}^2 \ll 1)$. (3.61)

The expression (3.61) differs from (3.47) for the non-inverting modulator by the factor $1-\gamma_{20}^2$. As can be seen from an examination of (3.57) and (3.61), when an increase in the parametric coupling increases the gain without limit, the bandwidth of the parametric amplifier tends to zero. The product of the voltage gain by the bandwidth is a constant quantity

$$\sqrt{K_-}\cdot 2\overline{\Delta\omega} = \omega_2\frac{\Delta C}{\sqrt{C_1 C_2}} \quad \text{for} \quad (1-\gamma_{20}^2) \ll 1.$$

Let us examine by way of an example the characteristics of an inverting modulator for the same signal frequencies in the preceding example and, for various values of γ_{20}^2, assuming $g_s g_{2L}/g_0^2 = 1$:

ν_1 = 100 Mcs, ν_2 = 20,000 Mcs, ν_0 = 21,100 Mcs.

γ_{20}^2	Gain, 10 log K_-, db	Bandwidth, $2\Delta\nu/k$, Mcs	Sensitivity, Sg
0,172	+23	1752	−1,414
0,90	+48,5	70,7	−19
0,99	+69	7,07	−199

When $\gamma_{20}^2 = 0.172$ we get $K_- = \omega_2/\omega_1$, as in the case of the non-inverting modulator. In this case the bandwidth is somewhat narrower than in the non-inverting modulator. Upon approaching self-excitation the inverting modulator may have a gain as large as desired, but its stability increases greatly. Thus, merely reducing the conductance by 1% or increasing the depth of modulation by an equal amount causes the circuit to oscillate if $\gamma_{20}^2 = 0.99$.

3. Parametric Amplifier with Negative Input Conductance

From an examination of an inverting modulator with differential combination frequency it follows that a reactive amplifier operating without conver-

sion of the amplified frequency is feasible. In such a device the amplification will be produced by the negative conductance introduced in the input circuit by the reactive modulator. The difference between such an amplifier and an amplifier with double (or multiple) pumping frequency is that the former is insensitive to the phase of the pumping generator of carrier frequency ν_0; moreover, the frequency of the signal need not be commensurate with the frequency of energy pumping.

It may appear strange that the phase relations between the signal and the variation of the parameter do not play any role whatever in this case, while in other parametric phenomena the phase relations are very important. In the mechanism of energy pumping the phase relations play a principal role in this case, too. Pumping will occur only under a suitable phase of the current at the corresponding combination frequency. But in a double-loop modulator the phase necessary for energy pumping is established automatically by a total frequency decoupling of the loops. Since the phase of the oscillations in the second loop can be arbitrary, it is automatically established such that, under given arbitrary signal phases and pumping-generator phases, a redistribution of the energy flow occurs in accordance with the general energy relations for nonlinear elements. This illustrates the need for the second loop, even if the amplified signal is taken only from the first loop. Energy consumption ($g_2 \neq 0$) must be insured in the second loop, or else the energy flow to the first loop and the negative resistance introduced in the first loop will be equal to zero. The presence of two loops is in itself insufficient to exclude the influence of the phase on the amplification factor. It is important that both loops be completely decoupled. In particular, if there are two loops, but $\omega_2 = \omega_1$ and $\omega_0 = 2\omega_1 = 2\omega_2$, then the first loop will not represent a short circuit to the frequency ω_2, nor will the second one to the frequency ω_1. In this case the two-loop system becomes degenerate. At small detuning

$$|\Delta\omega| = |\omega_c - \omega_1| \ll \omega_1$$

a voltage at a frequency $\omega_0 - \omega_S = \omega_1 - \Delta\omega = \omega_S - 2\Delta\omega$ will be present not only in the second loop but also in the first one, provided $2\Delta\omega$ is not far beyond the bandwidth of the first loop. This will produce beats of frequency $2\Delta\omega$. The same will occur in the second loop.

Let us consider an amplifier with a negative input resistance due to energy pumping in the first loop (Fig. 17). This circuit differs from that of the inverting regulator essentially in that the first

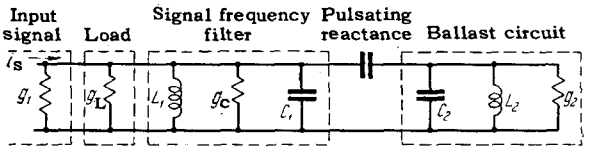

FIG. 17. Diagram of parametric amplifier with negative resistance.

signal loop contains an additional active load conductance g_L. In addition, account is also taken of the active component loop conductance, g_c, which includes also the loss (g) of the coupling capacitor. The general relations obtained above for the inverting modulator can be readily applied to the circuit of Fig. 17. In analogy with (3.51), the voltage across the first loop is given by the relation

$$\dot{U}_1 = \frac{1}{|\dot{Y}_{1\,eq}|^2}\dot{J}_s, \tag{3.62}$$

where

$$\dot{Y}_{1eq} = \dot{Y}_1(\omega_s) - \gamma_2^2\dot{Y}_2(\omega_0 - \omega_s).$$

But now $Y_1 = g_1 + g_c + g_L + j(\omega_S C_1 - 1/\omega_S L_1)$, i.e., it includes an additional load conductance g_L and the intrinsic conductance g_c of the loop. The power delivered to the load will be

$$P_L = |\dot{J}_s|^2 \frac{g_L}{|\dot{Y}_{1\,eq}|^2}.$$

The maximum signal power P_{in} will be as before

$$P_{in} = |\dot{J}_s|^2 \frac{1}{4g_1}.$$

The power gain K equals the ratio P_L/P_{in}

$$K = \frac{P_L}{P_{in}} = \frac{4g_1 g_L}{|\dot{Y}_{1\,eq}|^2}. \tag{3.63}$$

At exact tuning, $\dot{Y}_{1\,eq} = g_1 + g_c + g_L - g$ and (3.63) becomes

$$K_0 = \frac{4g_1 g_L}{(g_{1tot} - g)^2}, \tag{3.63'}$$

where $g = \gamma_2^2 g_2$ is the negative conductance introduced, and $g_{1\,tot} = g_1 + g_2 + g_L$ is the total conductance of the source, the first loop, and the load.

In a practical amplifier with negative input conductance it is desirable to connect the load through a unidirectional valve, or else the load noise will flow back to the amplifier and will return to the load in regenerated form. It is also advisable to apply the input signal through a unidirectional valve. This is done with a circulator/17/ in the centimeter band and with a balanced double-T network/18/ in the decimeter band.

Let us examine the circuit of Fig. 18, in which the circulator is connected between the signal generator and the input loop in such a way that the incident and reflected waves are separated. The power P_{inc} corresponds to the power delivered

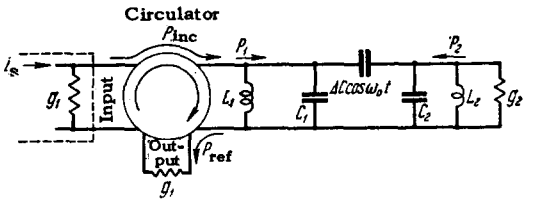

FIG. 18, Diagram of parametric amplifier with circulator for decoupling the input from the output.

by the signal source; P_{ref} is the power in the reflected wave, guided by the circulator towards the amplifier g_L, which is matched to the internal conductance of the signal source; P_1 and P_2 are the values of the power to the left and the right of the pulsating reactance (in our case both P_1 and P_2 are negative). The gain is given by

$$K = \frac{P_{ref}}{P_{inc}}.$$

The previously introduced definitions (3.54) and (3.55) now assume the following form

$$G_- = \frac{-P_2}{P_1}, \qquad K_- = \frac{-P_2}{P_{inc}}.$$

Since the power of the incident wave equals the sum of the reflected and transmitted power, i.e.,

$$P_{inc} = P_{ref} + P_1,$$

then

$$K = 1 - \frac{P_1}{P_{inc}} = 1 - \frac{K_-}{G_-}. \tag{3.64}$$

Inserting the values of K_-/G_- from (3.55) into (3.64) we get

$$K = 1 + \frac{4g_{ss}g_-}{|\dot{Y}_{1\,eq}|^2}\frac{g_L}{g_1}. \tag{3.65}$$

If a narrow-band amplifier is considered, we can use in (3.64) the expression given for K_- in (3.57). At $\gamma_{20}^2 \cong 1$ it is possible to neglect in (3.65) unity compared with the sufficiently large second term, and all the further calculations for the bandwidth of the inverting modulator can be applied directly to the amplifier with negative conductance.

4. Noise of Amplifier with Negative Conductance

The amplifying properties of modulators with reactive nonlinear elements can be used where an amplifier with low level of intrinsic noise is needed. The greatest interest attaches to this in the microwave region, where it is particularly difficult to reduce the noise of amplifying devices that employ free electron beams. The principal reason for the considerable noise of such amplifiers is the high temperature of the cathode that emits the electrons. Many papers[14,15,16] contain an analysis of the noise of parametric amplifiers. To conclude this section, we consider briefly the noise of an amplifier with negative conductance and a non-inverting modulator.

By definition the noise factor F is the ratio of the output noise power N_{out}, divided by the gain K, to the input noise power, N_{in}

$$F = \frac{N_{out}}{K \cdot N_{in}}. \tag{3.66}$$

In the case of a matched input, the input noise can be considered to be thermal noise and to obey the Nyquist formula

$$N_{in} = kT_0\Delta\nu, \tag{3.67}$$

where k is Boltzmann's constant, T_0 the standard absolute temperature (290°K), and $\Delta\nu$ the bandwidth. Let us assume that the gain in the bandwidth $\Delta\nu$ differs little from the resonant gain (3.63′) in an amplifier with negative conductance. Inserting (3.67) and (3.63′) into (3.66) we obtain

$$F = \frac{1}{4kT_0\Delta\nu}\frac{(g_{1tot}-g_-)^2}{g_1 g_L}N_{out}. \tag{3.68}$$

Thus, the determination of the noise factor reduces to a determination of the level of the output noise N_{out}. Reference 15 lists eight components of N_{out}, all assumed to be additive:

1. Thermal noise at frequency ω_1 of the first loop.
2. The same at frequency ω_2 in the second loop.
3. Noise current generated by the pulsating capacitance at frequency ω_1.
4. The same at frequency ω_2.
5. Noise at frequency ω_0, due to fluctuations in the amplitude ΔC of the pulsating capacitance.
6. The same at frequency $2\omega_1$.
7. The same at frequency $2\omega_2$.
8. The same at frequency $\omega_1 - \omega_2$.

We can thus rewrite (3.68) as

$$F = \frac{1}{4kT_0\Delta\nu}\frac{(g_{1tot}-g_-)^2}{g_1 g_L}\sum_{k=1}^{8} N_{k\,out}. \tag{3.68′}$$

To calculate $N_{1\,out}$ of the first output-noise component let us examine the equivalent circuit of the first loop (Fig. 19), obtained on the basis of the diagram in Fig. 17. Noise of frequency ω_1 is produced in the first loop by the conductance g_1 of the generator. The intrinsic noise of the load is not considered here, since the load is not included in the amplifier, although this noise may be of considerable intensity. The noise level, in accordance with the circuit of Fig. 19, will be

$$N_{1\,out} = \frac{i_1^2}{(g_{1tot}-g_-)^2}g_L = \frac{4kT_0\Delta\nu\,(g_1+g_c)}{(g_{1tot}-g_-)^2}g_L. \tag{3.69}$$

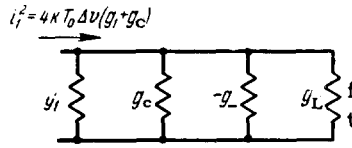

FIG. 19. Equivalent circuit for the conductance noise of the first loop.

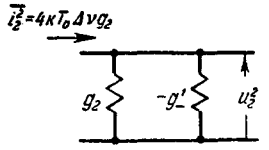

FIG. 20. Equivalent circuit for the conductance noise of the second loop.

Inserting (3.69) in (3.68′) we obtain the first component of the noise factor

$$F_1=1+\frac{g_c}{g_1}. \tag{3.70}$$

The second source of noise is the thermal noise in conductance g_2 of the second loop, at a frequency ω_2. The pulsating capacitance converts this noise to a frequency ω_1. The equivalent circuit for this noise is shown in Fig. 20. The noise is produced by the ballast network, g_2. The negative conductance $-g'_- = g_{1-}^2 - g_{1\,tot}$ is analogous to the negative conductance $-g_-$ introduced into the first network. The value of γ_{1-}^2 is, correspondingly,

$$\gamma_{1-}^2=\frac{\left(\frac{1}{2}\Delta C\right)^2\omega_1\omega_2}{g_{1\,tot}^2}=\gamma_{2-}^2\frac{g_2^2}{g_{1\,tot}^2},$$

and

$$g'_-=\left(\gamma_{2-}^2\frac{g_2^2}{g_{1\,tot}^2}\right)g_{1\,tot}=g_-\frac{g_2}{g_{1\,tot}}. \tag{3.71}$$

The mean squared noise voltage $\overline{u_2^2}$ in the second loop, in accordance with Fig. 20 and (3.71), is

$$\sqrt{\overline{u_2^2}}=\frac{\sqrt{\overline{i_2^2}}}{g_2-g'_-}=\sqrt{\overline{i_2^2}}\,\frac{g_{1\,tot}}{g_2(g_{1\,tot}-g_-)} \tag{3.72}$$

By analogy with (3.50) and (3.52), we can find the noise voltage $\sqrt{\overline{u_1^2}}$ of frequency ω_1 in the first loop, due to the noise voltage $\sqrt{\overline{u_2^2}}$ of frequency ω_2 on the pulsating capacitance $\Delta C\cos\omega_0 t$

$$\sqrt{\overline{u_1^2}}=\gamma_{1-}\sqrt{\frac{\omega_1}{\omega_2}}\cdot\sqrt{\overline{u_2^2}}=\sqrt{\frac{g_-}{g_2}\frac{\omega_1}{\omega_2}\frac{\overline{i_2^2}}{g_{1\,tot}-g_-}}. \tag{3.73}$$

The second component of the output noise, $N_{2\,out}$ is, in accordance with Fig. 20 and (3.73),

$$N_{2\,out}=g_L\overline{u_1^2}=4kT_0\Delta\nu\frac{gg_L}{(g_{1\,tot}-g_-)^2}\frac{\omega_1}{\omega_2}, \tag{3.74}$$

and the noise factor is

$$F_2=\frac{\omega_1}{\omega_2}\frac{g_-}{g_1}. \tag{3.75}$$

In analyzing the third component of the output noise, $N_{3\,out}$, we should return to the equivalent circuit of the first loop, Fig. 19, and replace the current $\overline{i_1^2}$ by a noise current of frequency ω_1, generated by the pulsating capacitance. We denote this current by $\overline{i_3^2}$. This latter current cannot be determined from the amplifier parameters introduced so far. It is caused by the nature and mechanism of the pulsating capacitance, as are all the remaining components. In particular, if the capacitance is varied electronically, $\overline{i_3^2}$ corresponds to the shot-noise current. This noise is substantial in electron-beam devices and is vanishingly small if a semiconductor with negative bias is used as the pulsating nonlinear capacitance. Without evaluating $\overline{i_3^2}$, we can write

$$N_{3\,out}=\frac{\overline{i_3^2}}{(g_{1\,tot}-g_-)^2}g_L \tag{3.76}$$

and

$$F_3=\frac{\overline{i_3^2}}{4kT_0\Delta\nu g_1}. \tag{3.77}$$

We shall not consider the remaining components of the noise factor, for they cannot be estimated effectively without stating the concrete type of amplifier used. The resultant noise factor (3.68) can be written

$$F=1+\frac{g_c}{g_1}+\frac{\omega_1}{\omega_2}\frac{g_-}{g_1}+\frac{\overline{i_3^2}}{4kT_0\Delta\nu g_1}+\text{ terms due to shot noise and fluctuations in the pulsating reactive element.} \tag{3.78}$$

For the solid-state variant of the parametric amplifier, apparently only the first three terms of (3.78) are important, including the unity term. The ratio g_c/g_1 is very small. The third term of the noise factor, due to the ballast network, is more substantial and approaches ω_1/ω_2 at high gains. But by choosing $\omega_2 \gg \omega_1$ the third term can be made sufficiently small. If the loop temperature is reduced by forced cooling, the second and third term of (3.78) should be multiplied by T/T_0, where T is the actual loop temperature.

It is interesting to estimate the minimum value of the noise factor. For this purpose we return to the amplifier circuit with circulator and matched load $g_L = g_1$ (Fig. 18). The resultant loop conductance should be $g_1 + g_c$, since the load and generator conductances each act only in one direction. At large gain the negative conductance g introduced is close to $g_1 + g_c$. Taking these circumstances into account and neglecting all terms but the first three, we can rewrite (3.78) in the following form:

$$F\cong 1+\frac{g_c}{g_1}+\frac{\omega_1}{\omega_2}\frac{g_1+g_c}{g_1}. \tag{3.79}$$

Since the carrier frequency satisfies the equation $\omega_0 = \omega_1 + \omega_2$, then

$$F\cong\frac{\omega_0}{\omega_2}\frac{g_1+g_c}{g_1}. \tag{3.80}$$

If the coupling between the generator and the amplifying network is large, the ratio $(g_1+g_c)/g_1$ can be made close to unity and the noise factor reaches a minimum, the value of which is

$$F = \frac{\omega_0}{\omega_2}. \quad (3.81)$$

It must be borne in mind that the losses in the pulsating reactance are accounted for in g_c. In the determination of the minimum of the noise factor, the circulator is assumed to produce no noise.

The noise factor of the non-inverted modulator, F_+, determined in an analogous manner, is

$$F_+ = 1+\frac{\alpha}{\sqrt{1+\alpha^2}}\left[1+\frac{\omega_1}{\omega_2}\left(\alpha+\sqrt{1+\alpha^2}\right)^2\right]\frac{T}{T_0}, \quad (3.82)$$

where $\alpha = \tan\delta_p$, in accordance with (3.49); the gain in (3.66) is determined from (3.48). The minimum of F_+ will not occur at the maximum gain (3.66). If K_+ is specified, the noise factor can be reduced, by suitable choice of g_s, to

$$(F_+)_{\min} = 1+2\alpha^2\frac{\omega_1}{\omega_2}\left(1+\sqrt{1+\frac{\omega_2}{\omega_1\alpha^2}}\right)\frac{T}{T_0}. \quad (3.83)$$

Reference 16 contains the calculation of $(F_+)_{min}$ for a coupling capacitor in the form of semiconductor diode, with losses accounted for. At a signal frequency $\nu_1 = 500$ Mcs and a carrier frequency $\nu_0 = 10{,}000$ Mcs we get $(F_+)_{min} = 1.32$, whereas $(F_+)_{min} = 1.66$ at $\nu_1 = 1{,}000$ Mcs. These results are in satisfactory agreement with experiment (see reference 22).

4. NEW TYPE OF NONLINEAR CAPACITANCE —THE CRYSTAL DIODE

As indicated in the introduction, capacitance can be changed not only by varying the dielectric constant in the capacitor, but by changing the distance between charges on the opposite sides of the capacitor. Recently the method of changing the distance between charges has found embodiment in the use of the capacitance of a p-n junction of a crystal diode.

At the junction of p and n type semiconductors there is formed a so-called barrier layer, owing to recombination of the mobile carriers of one polarity with the diffusing carriers of the opposite polarity. In the equilibrium state, the distribution of the concentrations of the carriers — holes and electrons — about the p-n junction is as shown in Fig. 21a. In the capacitor produced by the p-n junction, the role of the dielectric is played by the barrier layer itself, in which there are practically no moving carriers; the role of the electrodes are played by the p and n regions adjacent to the barrier layer, which have normal electric conductivity.

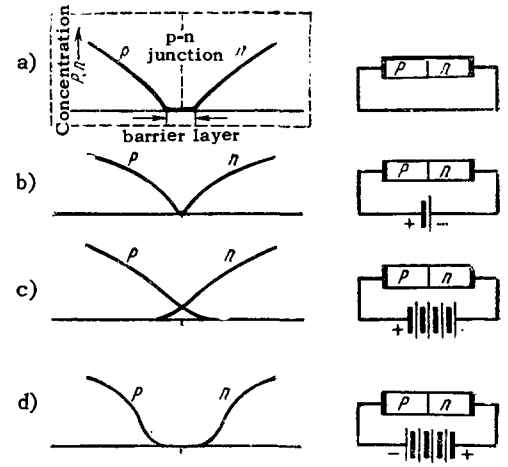

FIG. 21. Diagram showing the variation of the thickness of the blocking layer of a junction with voltage. a – zero bias, b – small forward bias, c – forward bias, d – reverse bias.

The width of the barrier layer of a p-n junction in equilibrium increases with increasing potential barrier of the junction, and is determined by the resultant contact potential difference at the junction. For germanium, the resultant contact potential difference of the p-n junction ranges from 0 to 0.7 volts. If a small voltage is applied to the p-n junction in the forward direction, i.e., with the plus terminal connected to the p-region, then the potential barrier is reduced and the barrier layer becomes narrower, as shown in Fig. 21b. The capacitance of the junction increases. If the direct voltage is increased still more, considerable mixing of electrons and holes occurs, both in the barrier layer as well as on both sides of it (Fig. 21c). In spite of the mixing, the moving carriers can return to their regions without recombination, if the recombination time is large compared with the duration of the period of variation of the applied voltage. Experience has shown that recombination is negligible if the frequency of the applied voltage is much higher than 1 Mcs. The nonlinear capacitance produced thereby is called "diffusion" or "stored-charge" capacitance. At low frequencies it is shunted by the relatively-large conductance of the p-n junction in the forward direction.

If a voltage of reverse polarity is applied to the junction, with the minus connected to the p region, then the barrier layer broadens, as shown in Fig. 21d. The capacitance of the junction decreases. The minimum capacitance obtainable is limited by the breakdown voltage, for when the inverse voltage applied to the p-n junction exceeds the breakdown voltage, large conduction is produced because of the cascading process of gen-

eration of mobile carriers in the barrier layer, and the diagram of 21d no longer holds. In the range of voltages from the negative breakdown voltage to the small positive voltage, not exceeding the resultant contact difference of potentials on the p-n junction (Fig. 21b), the displacement of the mobile carriers is not accompanied by a considerable mixing of the carriers. The nonlinear capacitance that is produced thereby is called "static" or "barrier-layer" capacitance. This capacitance is practically independent of the frequency, whereas the diffusion capacitance depends greatly on the frequency. Generally speaking, the static capacitance also has a dispersion, but only in the region of very high frequencies. This dispersion has not been observed experimentally as yet. Calculations show it to be in the 10^{12} cps ($\lambda = 0.3$ mm) region. It is here that advantage of the electronic nature of the nonlinear capacitance over the domain nature is manifest. The invention of the semiconductor nonlinear capacitor belongs to B. M. Vul (1954). References 19 and 20 give the equivalent circuit of the p-n junction (Fig. 22), characteristic curves for the dependence of the capacitances of fused-junction and diffusion diodes on the reverse bias, and a discussion of the principles of nonlinear semiconductor capacitors. Later foreign articles contain analogous calculations and consider the application of semiconductor capacitors without any references whatever to these papers.*

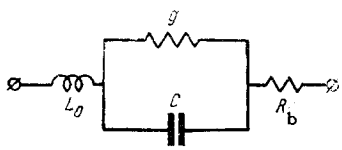

FIG. 22. Equivalent circuit of crystal diode used as as a nonlinear capacitor.

The losses in a nonlinear capacitor are determined by the active conductance. Figure 22 shows the equivalent circuit of a nonlinear capacitor in the form of a junction germanium diode at microwave frequencies as described by Giacoletto and O'Connell.[21]. This equivalent circuit was found to be valid for a very broad range of frequencies from 1 to 800 Mcs. The inductance L_0 includes that of the leads. In the specimen described it amounted to $L_0 = 2.6 \times 10^{-3}\,\mu h$. To reduce L_0, the leads were made short and thick.

The base resistance R_b includes the resistance in the layer of n-germanium between the contact of the base and the surface of the barrier layer of the junction. The quality of a nonlinear capacitor used at microwave frequencies is determined by the upper critical frequency

$$\nu_B = \frac{1}{2\pi R_b C_{min}}, \qquad (4.1)$$

where C_{min} is the lowest attainable value of the nonlinear capacitance. The base resistance R_b is inversely proportional to the area of the junction, and the capacitance C is directly proportional to this area; therefore ν_u is independent of the junction area. To increase ν_u the base should be made as thin as possible and its conductance made sufficiently high. The conductance of the base is determined by the concentration of impurities, which in turn is related to the breakdown voltage. In the sample described $R_b = 0.5$ ohms, the breakdown voltage is approximately -16 v and $\nu_u \approx 10{,}000$ Mcs.

The size of the capacitance is determined by the junction area, which in this case is determined by the contact surface of the indium point fused into the n-germanium. The capacitance C in the sample described ranged from 79 to 24.5 $\mu\mu$f for a reverse bias ranging from -1 to -15 volts. The connection between the capacitance C and the voltage u applied to the junction varies with the character of variation of the concentration of acceptors and donors in the p-n junction. If this variation is linear (diffusion diode), then

$$C \sim \frac{1}{\sqrt[3]{1-\frac{u}{\varphi}}} \qquad (4.2)$$

In the case of a sharp and ragged variation of concentration (in a fused diode) we have

$$C \sim \frac{1}{\sqrt{1-\frac{u}{\varphi}}}, \qquad (4.3)$$

where p is the contact difference of potential (approximately 0.5 v). The diode discussed here obeyed relation (4.3). The relative change in capacitance, $\Delta C/C$, can be determined from (4.3):

$$\frac{\Delta C}{C} = \frac{1}{2}\frac{\Delta u}{\varphi - u}. \qquad (4.4)$$

As follows from (4.4), $\Delta C/C$ is independent of the diode dimensions, and at large values of u it is also independent of the material of the diode (of φ)

$$\frac{\Delta C}{C} \cong -\frac{1}{2}\frac{\Delta u}{u} \quad \text{for} \quad |u| \gg \varphi. \qquad (4.5)$$

The junction capacitance C is shunted by the leakage conductance g, which is due to thermal generation and recombination of mobile carriers.

*In Author's Certificate (patent disclosure) No. 110441, issued to B. M. Vul for the invention of "Semiconductor Nonlinear Capacitors," with priority date June 29, 1954, the object of the invention is stated as follows: "The use of semiconductor diodes and triodes as semiconductor nonlinear capacitors, in which the change of capacity is effected by changing the voltage on a diode, and by changing the collector voltage or the emitter current in triodes." Along with semiconductor diodes, transistors are also finding use as controllable nonlinear capacitors.

The quality of the nonlinear capacitance in the low-frequency range is determined by the lower critical frequency ν_l

$$\nu_l = \frac{g}{2\pi C_{max}}, \qquad (4.6)$$

where C_{max} is the highest attainable value of the nonlinear capacitance. In the specimen described $g \approx 5 \times 10^{-8}$ mho and $\nu_l = 10{,}000$ cps. Figure 23 shows the geometry of the described diode, while Fig. 24 shows the dependence of the capacitance on the reverse bias. It is interesting to note that there is an optimum frequency, at which the Q of the capacitor has a maximum. The maximum Q of the capacitor described here was 3,000, albeit at a relatively low frequency, 1 Mcs.

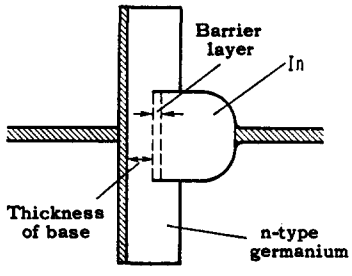

FIG. 23. Geometry of a crystal diode used as a nonlinear capacitor.[21] Thickness of germanium slab 0.05 mm, dimensions of indium bead 0.5 mm.

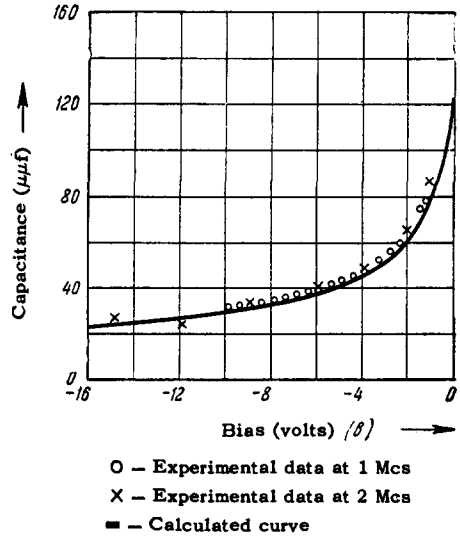

FIG. 24. Capacitance of crystal diode as a function of the reverse bias.[21]

Other types of nonlinear capacitors for microwaves are described in reference 22. In particular, a "flat top" diffusion silicon diode (Fig. 25) has a capacitance-voltage curve as shown in Fig. 26. The same paper[22] mentions a germanium diode with a fused junction, alloyed with gold, in which the critical upper frequency reaches 40,000 Mcs. Mass production of germanium diodes for parametric amplifiers, with critical frequency of 70,000 Mcs, has been reported.

The question of shot noise due to the electron conductivity of the p-n junction is considered in reference 24 as applied to parametric amplifiers.

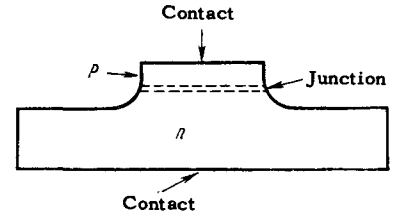

FIG. 25. Geometry of "flat top" crystal diode.[22]

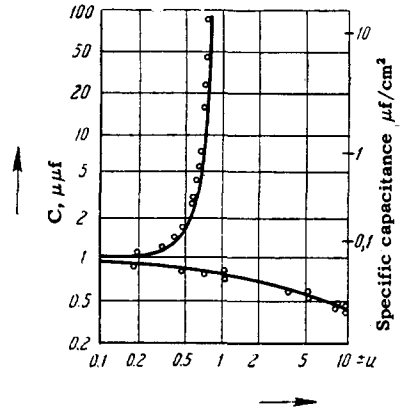

FIG. 26. Dependence of the capacity of the p-n junction of a "flat-top" diode on the bias voltage.[22]

+u) change in capacitance with increasing forward bias on the junction; −u) change in capacitance with increasing reverse bias; □ – experimental data at 100 kcs, o – experimental data at 1,000 Mcs.

5. CERTAIN NEW APPLICATIONS OF NONLINEAR REACTIVE ELEMENTS

With the appearance of high-Q nonlinear capacitors for microwaves, new prospects have opened up for the production of reactive amplifiers for this frequency range. Since such amplifiers do not contain hot cathodes, the level of the intrinsic noise can be made quite low. Furthermore, the parametric amplifier does not require a very low temperature for its operation as does the maser, and consequently it is much simpler to service. The June 1958 issue of the Proceedings of the IRE contains several preliminary communications on experimental models of various parametric amplifiers.

1. Reactive Broadband Amplifier with Low Noise Level[25]

The diagram is shown in Fig. 27. It differs from the ordinary balanced dielectric amplifier only in that the power is drawn at one (upper) sideband frequency. The two nonlinear capacitors used were typical silicon diodes with more or less similar parameters. The basic characteristics of this am-

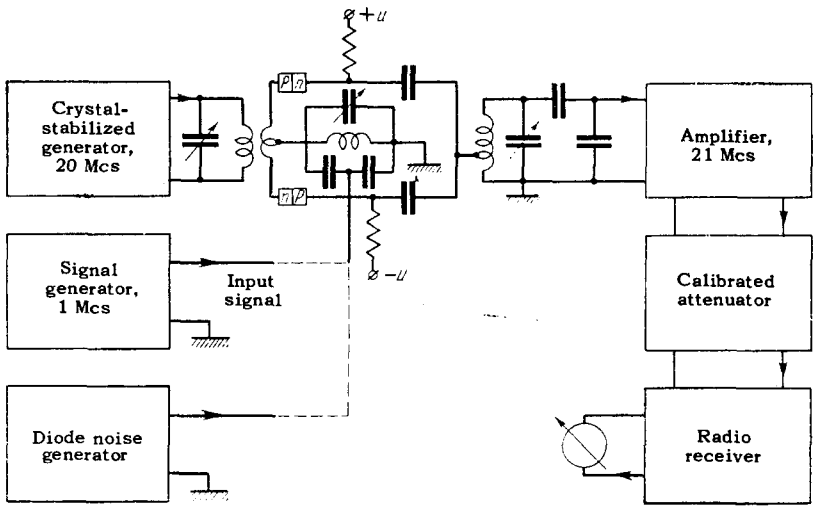

FIG. 27. Diagram of low-noise reactive amplifier for 1 Mcs.[25]

plifier are listed in the following table:

Signal frequency	1 Mcs
Carrier frequency	20 Mcs
Output frequency	21 Mcs
Relative bandwidth at input	10%
Power gain bandwidth at input	10 db
Effective noise temperature of amplifier	30°K
Total effective temperature	40°K

The effective noise temperature was determined from the formula $T_{eff} = T_0(F-1)$, where F is the noise factor and T_0 the standard temperature, 290°K. The diodes were kept at room temperature. Additional measurements, carried out with the input loop cooled with liquid nitrogen, have shown that the thermal noise of this loop amounts to a large fraction of the intrinsic noise.

2. Experimental Characteristics of a Microwave Parametric Amplifier with a Semiconductor Diode[26]

The amplifier is built as an inverting modulator. The problem of constructing filters for the necessary signal, carrier, and resonant frequencies, (ν_S, ν_0, and $\nu_0 - \nu_S$) was cleverly solved by using a rectangular cavity (Fig. 28). Using three modes, TE_{103}, TE_{301}, and TE_{101}, in a rectangular wave guide with a capacitive diode in the center portion, the authors have succeeded in obtaining the following three resonant frequencies:

$\nu_1 = 1200$ Mcs, $\nu_0 = 3500$ Mcs, and $\nu_2 = \nu_0 - \nu_1 = 2300$ Mcs.

The diode capacitance was modulated by pumping energy from a local generator of frequency ν_0 into the cavity with the aid of a coupling loop. The input and output at frequencies ν_1 and ν_2 were through two probes. The specially developed germanium junction diode had a capacitance of 1 $\mu\mu$f at zero bias (at low frequency) and a base resistance of 5 ohms.

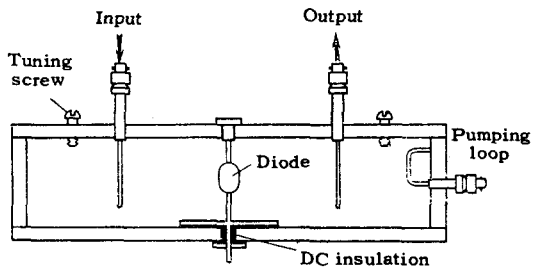

FIG. 28. Diagram of microwave parametric amplifier.[26]

At a pumping power up to 100 mw at $\nu_0 = 3500$ Mcs, oscillation was induced at the two frequencies, 1200 and 2300 Mcs. At lower pumping power it was possible to obtain amplification at each of the frequencies, ν_1 and ν_2. Most measurements were carried out in the amplifying mode at a frequency ν_1 with a negative bias of approximately 5 volts.

Gains up to 40 db could be obtained, although at such a high amplification the device became extremely sensitive to load variations, since the circuit did not include a decoupling insulator or circulator. Furthermore, a noticeable fluctuation was observed in the gain, owing to the residual frequency modulation of the pumping generator, the output of which was connected to a traveling-wave tube and a filter. The band width was 1.0 Mcs at a gain of 19 db; the product of the voltage gain by the bandwidth was constant, in accordance with the known rule. The greatest output power was 1.5 mw and the dynamic range more than 100 db. Preliminary measurements of the noise factor gave a value not exceeding 4.8 db at a gain of 16 db.

3. Measurements of the Noise Factor of Two Pulsating-Reactance Amplifiers with Semiconductor Diodes[27]

Herrmann et al. report[27] briefly on experiments with two types of parametric amplifiers: a non-inverting modulator and a negative-resistance amplifier.

The diagram of the non-inverting modulator is shown in Fig. 29. The frequencies of the output signal, the modulator carrier signal (ν_0) and the output signal ($\nu_2 = \nu_0 + \nu_1$) are 460, 8,915, and 9,375 Mcs respectively. The modulator output signal is fed to a measuring superheterodyne receiver. The gain of the modulator is 9 db. The noise factor is 2 ± 0.5 db, corresponding to a noise temperature of $170 \pm 50°$K. No special measures were undertaken to match the pumping generator to the reactive converter.

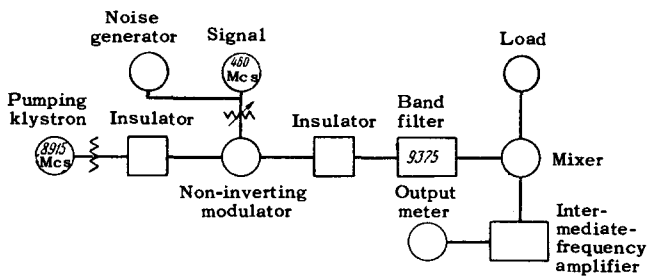

FIG. 29. Block diagram of parametric amplifier with summary combination frequency.[27]

Under very careful tuning (which could not be repeated immediately) a gain of 21 db and a total noise factor of 1.1 ± 0.5 db ($87 \pm 40°$K) were obtained. So high a gain exceeds the ratio $\nu_2/\nu_1 = 9375/460$. Apparently, the difference-frequency ($\nu_0 - \nu_1$) oscillations were not suppressed sufficiently.*

The negative-resistance amplifier is shown schematically in Fig. 30. The input signal frequency was 6,000 Mcs and the pumping frequency 11,700 Mcs. The input and output waves were separated by a circulator. Furthermore, the circulator kept the thermal noise of the load out of the amplifier. The nonlinear capacitances used were fused-contact silicon and germanium diodes, alloyed with gold. The diode capacitance C, in the absence of bias, was $0.4 - 2.85\ \mu\mu$f. The silicon diodes were used without bias, but a negative bias of 1.0 to 1.5 volt was applied to the germanium diodes to reduce the capacitance to a value suitable for optimum amplification.

*In particular, difference-frequency oscillations could develop in the circuit made up of the base resistance and the parasitic inductance of the semiconductor diode, which in this case serve as a ballast network for the difference-frequency oscillations.

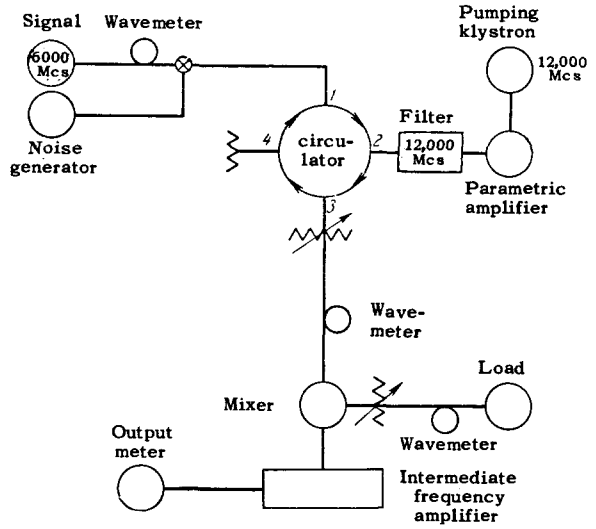

FIG. 30. Block diagram of parametric amplifier with negative resistance.[27]

A stable gain of 45 db was obtained at a signal frequency equal to half the pumping frequency ($\nu_1 = \nu_0/2$). The product of the bandwidth by the gain was found to be constant. When tuned for maximum gain of 18 db at $\nu_1 = \nu_0/2$ (10 Mcs), a bandwidth of 8 Mcs was obtained at the 3-db level.

The parametric method of amplification leads in this case to an appearance of the following noise components in the signal band: 1. Input noise of frequency ν_1, amplified together with the input signal. 2. Input noise of frequency $\nu_0 - \nu_1$, which is converted to ν_1 in the amplification process. 3. Diode noise of frequency ν_1. 4. Diode noise of frequency $\nu_0 + \nu_1$, which is converted into $\nu_0 - \nu_1$ in the amplification process.

To reduce the noise, it is useful to amplify a signal with two symmetrical sidebands, for which the central frequency is exactly equal to half the pumping frequency ($\nu_1 = \nu_0/2$). In this case, coherence between the components of the signal spectrum and the corresponding $\nu_0 - \nu_S$ will be maintained. With bands of such symmetry, the noise factor was 3 db, compared with 6 db in simple amplification. But as the equivalent temperature of the input load is reduced, the noise factor becomes less than 6 db even in simple amplification. The most important source of diode noise is the base resistance R_b. Analysis has shown that to reduce this noise it is necessary to strive for a reduction of the product $q = \nu_1 R_b C$. This premise was confirmed by tests of many diodes used in the negative-resistance amplifier. It should be noted that in a non-inverting amplifer operating at 400 Mcs the noise factor is considerably less than in a negative-resistance amplifier operating at 6,000 Mcs. It can be concluded from this, in

particular, that the noise generated in a non-inverting modulator at a frequency $\nu_0+\nu_1$ [where $\nu_0+\nu_1 \gg \nu_1$, and consequently also $q(\nu_0+\nu_1) \geq q(\nu_1)$] is not as great as the noise at ν_1, for the latter is amplified in the modulation process.

Heffner[35] believes that a parametric amplifier for the centimeter range is feasible with a noise factor of 0.5 db, i.e., with an equivalent noise temperature of 40° K with all the amplifier elements kept at room temperature (without cooling).

At the Third All-Union Conference on Radio Electronics of the U.S.S.R. Ministry of Higher Education, held in Kiev on January 23, 1959, V. S. Étkin and E. M. Gershenzon described a parametric amplifier developed and tested in the Laboratory of the Faculty headed by Prof. N. N. Malov at the V. I. Lenin Moscow State Pedagogical Institute. The wavelength high-frequency signal was 6 to 7 cm, and the pumping generator operated at 3.0 — 3.5 cm. Both amplification and generation were possible with ordinary microwave crystal diodes.

4. Parametric Electron-Beam Amplifier

It is interesting to note that the intrinsic noise in an amplifier with a free electron beam can be considerably reduced if a parametric mechanism of amplification is used. Bridges[28] describes a parametric electron-beam amplifier, the circuit of which is shown in Fig. 31. The resonator tuned to the signal frequency ν_s is coupled through two apertures with the electron beam, which moves uniformly past the apertures. If the transit angle α between the aperture is

$$\alpha = \left(2n+\frac{3}{2}\right)\pi, \quad n=0,\ 1,\ 2,\ \ldots,$$

then the electron beam produces in the resonator a purely-negative resistance. The negative resistance produced by the beam compensates for the damping in the cavity of the resonator and can induce generation.

On the other hand, if the transit angle α is made one quarter of a period greater or smaller than the value indicated above, the beam will induce in the resonator a pure reactance:

$$\alpha = (2n+1)\pi \quad \text{for positive reactance,}$$
$$\alpha = (2n+2)\pi \quad \text{for negative reactance.}$$

This beam-induced reactance changes the resonant curve of the cavity without changing the damping. If the electron beam is now modulated and oscillations are excited in the resonant pumping cavity (see Fig. 31), this will result in modulation of the reactance parameter in the signal resonator. The optimum distance between resonators necessary for

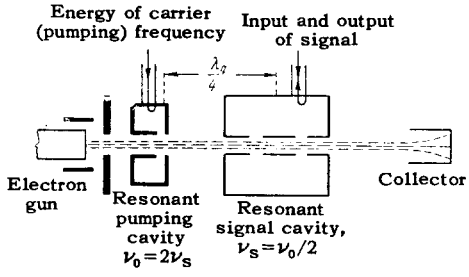

FIG. 31. Diagram of electron-beam parametric amplifier.[28]

production of a density-modulated beam is one-quarter the effective plasma wavelength.

At a pumping frequency equal to twice the signal-resonator frequency, parametric pumping of energy occurs into the signal-resonator tank circuit, i.e., the amplifier described is a realization, for the microwave band, of the single-loop parametric amplifier, the principle of which, except for the modulated electron beam and the new technology, was suggested in the thirties by the school of Mandel'shtam and Papaleksi.[6]

A valuable feature of the parametric electron-beam amplifier is that even at a high level of shock noise in the electron beam, the noise level induced in the resonator is low. Since the distance between the resonator apertures is small compared with the plasma wavelength, the beam current at the apertures is in the first approximation of equal amplitude and opposite phase, provided the transit angle is

$$\alpha = (2n+1)\pi.$$

In other words, by choosing transit angles of π, 3π, 5π, etc. it is possible to effect parametric amplification without, in the first approximation, coupling of the signal resonator to the noise component of the electron-beam current.

In the experimental setup corresponding to Fig. 31, both amplification and generation of oscillations were observed at a sufficiently deep beam modulation. The noise was not measured. The table lists certain of the measured characteristics:

Signal Resonator	
Resonant frequency ν_s	4150 Mcs
Transit angle α	3π radians
Pumping frequency ν_0	8300 Mcs
Beam voltage	2,450 v
Beam current	18 ma
Pumping power	140 mw
Maximum gain	20 db

Figure 32 shows oscillograms of the output signal at a swinging input-signal frequency and at various levels of pumped energy, with continuous gener-

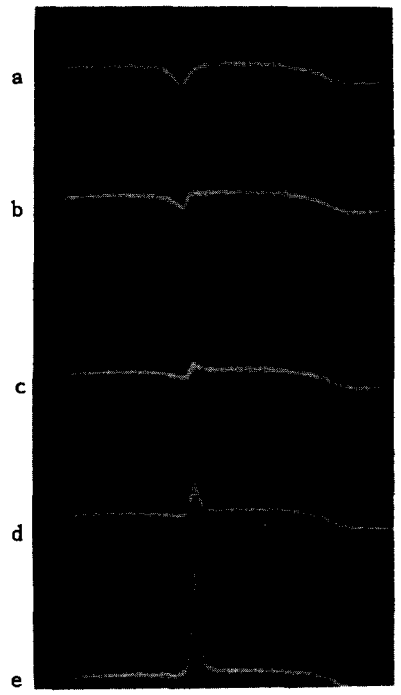

FIG. 32. Oscillograms showing the dependence of the amplification on the pumping power.[28]

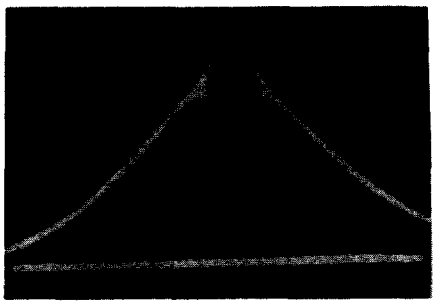

FIG. 33. Fluctuations of the gain upon change in phase relations in an amplifier with a multiple pumping frequency.[28]

ation at a fixed frequency ν_0. In the case of Fig. 32a, the pumped energy was zero, and the electron beam was not modulated. At the resonant frequency a reduction was observed in the amplitude of the signal fed to the amplifier from the swinging klystron. The input and output of the amplifier were not decoupled, and the oscillogram showed the usual sharp increase in energy absorbed by the cavity at the resonant frequency. The oscillogram of Fig. 32b shows the reduction in attenuation in the resonator, and was plotted at a pumping power of 35 mw. The oscillograms of Figs. 32c to 32e were taken at pumping powers of 56, 82, and 140 mw respectively.

In this degenerate parametric amplifier, the phase relations between the signal and the parameter modulation are important. During the frequency swing of the signal, these phase relations vary continuously, and the gain fluctuates correspondingly between the maximum value of the "strong" and the lowest value of the "weak" resonance. If a detector of sufficiently low inertia is used at the output, such gain fluctuations can be observed. The oscillogram of Fig. 33 shows a band of gain oscillations, obtained in the same mode as the oscillogram of Fig. 32e, but with a low-inertia detector on an enlarged scale.

Another electron-beam parametric amplifier is reported in reference 29.

In addition to the foregoing applications of high-frequency nonlinear reactance in parametric amplifiers, such reactances can be used also in a variety of other devices for frequency conversion, generation of harmonics, or generation of subharmonics. But this does not exhaust all the possibilities of nonlinear reactance elements. A very instructive example is the use of nonlinear capacitance in conjunction with a nonlinear resistance in a trigger circuit.[30,31] Figure 34 shows a circuit with two positions of stable equilibrium.

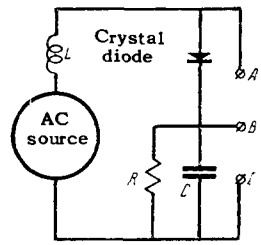

FIG. 34. Trigger circuit with two stable states.[30]

The tank circuit, comprising an inductance L in series with the capacitance C_d of the semiconductor diode, is fed from a high-frequency ac source. The diode described in reference 21 was used in this circuit. The parallel RC network is a filter for the dc component due to the rectifying action of the semiconductor diode. The capacitance C is considerably greater than C_d, and the time constant of the RC filter exceeds by many times the period of the high frequency voltage applied to the tank circuit. The ratio of the input-voltage period T to the tank-circuit period $T_0 = 2\pi\sqrt{LC_d}$ is chosen such as to satisfy the following inequality in the absence of bias:

$$T_0 > T,$$

and to the contrary, in the case of a large inverse bias:

$$T_0 < T.$$

The rectified output voltage in the circuit of Fig. 34 (between terminals B and C) is simultaneously the inverse bias for the semiconductor diode. As the amplitude of the input voltage changes, the rectified voltage across terminals BC will vary as shown in Fig. 35. As the amplitude is increased from zero, a corresponding almost linear increase

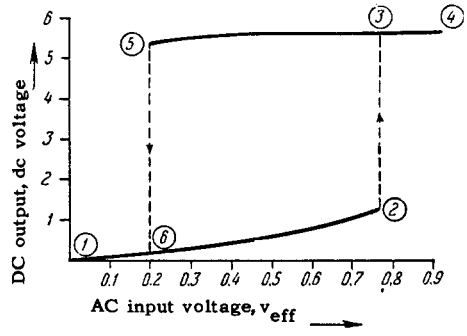

FIG. 35. Diagram showing the dependence of the output dc voltage at terminals BC on the alternating input in the circuit of Fig. 34.

in voltage will be observed (curve 1 — 2 of Fig. 35). This will continue until the decrease in C_d will cause resonance of the tank circuit LC_d. On approaching resonance, the ac voltage on C_d will begin to increase rapidly, and the dc component of the voltage on RC will also increase, causing a further decrease in C_d and a corresponding further approach to resonance. This results in an avalanche-like jump in variation of the output voltage (section 2 — 3 of Fig. 35). The output voltage changes little with further increase in the input voltage. Moving back along the curve of Fig. 35, an avalanche-like decrease in the output voltage occurs at point 5. At input voltages ranging from 0.2 to 0.7 volt, the circuit had two stable equilibrium positions. A sudden increase in input voltage to 0.75 volt shifts the system to the upper level of the output voltage, while reduction of the output voltage to 0.15 volts returns it to the lower level. The system flip could also be realized by other means, such as changing the bias or changing the frequency of the input voltage. Figure 36 shows a variation of the output rectified voltage in the circuit of Fig. 34 as the input voltage is varied. Under suitable conditions, the circuit can be triggered by light incident on the p-n junction. Using several series elements of the type shown in Fig. 34 and adding feedback, it is possible to construct multivibrators and the like.

Generally speaking, a trigger circuit with a nonlinear resonance loop can be realized also by

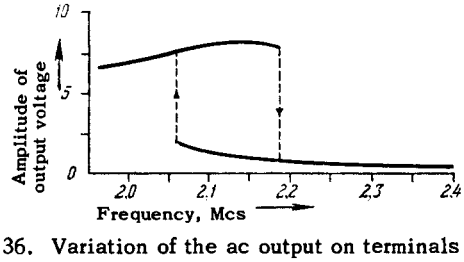

FIG. 36. Variation of the ac output on terminals ac with the frequency of the ac input voltage in the circuit of of Fig. 34.

using other reactive nonlinear elements, such as coils with ferromagnetic cores or capacitors with ferroelectrics, and not only a crystal diode. But in the latter case there is assurance of good high-frequency performance and easy manipulation. In particular, by using in Fig. 34 an ac source of frequency 2.2 Mcs, C = 330 $\mu\mu$f, R = 500,000 ohms, and an adjustable inductance L = 64 to 105 μh flips of 2 μsec approximate duration were obtained. It must be noted that a reduction in the capacitance C or an increase in the frequency of the ac source reduce the duration of the leading front, but hardly affect the duration of the trailing edge. Very large values of R, while sharpening the leading front, cause a prolonged slow trailing edge.

The circuit of Fig. 34 can be improved by using two identical diodes in a balanced circuit, and also by using a transistor as two diodes with nonlinear capacitances and conductances.

CONCLUSION

We have considered by far not all aspects of the application of reactive nonlinear elements, and have touched only upon some of their characteristic properties. Our aim was to call the attention of large groups of scientific workers engaged in electronics or making use of electronics, to nonlinear reactance elements and particularly to parametric systems, and to call their attention to the developing possibilities of employing such systems in certain devices in lieu of the more cumbersome, more complex, and less reliable vacuum-tube devices, and also to solve new problems in technology of amplification, modulation, control, etc. A very important factor in the development of reactive nonlinear elements is the devising and investigating of the new readily-controlled, reactive elements of high Q and low inertia. In particular, work is being done on the use of ferromagnetic resonance phenomena in parametric systems.[32,33,34,35] Oscillations in such systems are analogous to those in the reactive modulators considered here, but are also subject to many physical peculiarities of the behavior of ferromagnets in microwave fields.

[1] A. A. Fel'dbaum Введение в теорию нелинейных цепеи (Introduction to Theory of Nonlinear Networks), M-L., 1948.

[2] Melde, Pogg. Ann. **109**, 5 (1859); **111**, 513 (1860).

[3] Rayleigh, Phil. Mag. **229**, April (1883).

[4] Mandel'shtam, Papaleksi, Andronov, Vitt, Gorelik, and Khaĭkin Новые исследования нелинейных колебаний (New Investigations of Nonlinear Oscillations), M., 1936.

[5] L. I. Mandel'shtam and N. D. Papaleksi, J. Tech. Phys. (U.S.S.R.) **4**, 5 (1934). N. D. Papaleksi, Электричество (Electricity), No. 11, 67 (1938).

[6] L. I. Mandel'shtam and N. D. Papaleksi ИЭСТ No. 3, 1 (1935).

[7] L. I. Mandel'shtam and N. D. Papaleksi, J. Tech. Phys. (U.S.S.R.) **3**, 1141 (1933).

[8] G. S. Gorelik, J. Tech. Phys. (U.S.S.R.) **4**, 1783 (1934); **5**, 195 and 489 (1935); Techn. Phys. of the U.S.S.R. **2**, 135 (1935).

[9] L. I. Mandel'shtam Полное собрание трудов (Collected Works), II, papers 53 and 55, U.S.S.R. Acad. Sci., 1947.

[10] N. D. Papaleksi, J. Phys. Acad. Sci. (U.S.S.R.) **1**, 373 (1939). (Collected Works, paper 13, Acad. Sci. 1948).

[11] J. M. Manly and H. E. Rowe, Proc. IRE **44**, No. 7, 904 (1956).

[12] V. E. Bogolyubov, Электричество (Electricity) No. 6, 42 (1949).

[13] H. E. Rowe, Proc. IRE **46**, No. 5, 850 (1958).

[14] S. Bloom and K. Chang, RCA Rev. **18**, December 578 (1957).

[15] H. Heffner and G. Wide, J. Appl. Phys. **29**, No. 9, 1321 (1958).

[16] D. Leenov, Bell Sys. Tech. J. **37**, No. 4, 989-1008 (1958).

[17] Fox, Miller, and Weiss, Properties of Ferrites and their Use in the Microwave Band (Russ. Transl. "Soviet Radio" Press, M., 1956.)

[18] S. H. Autler, Proc. IRE **46**, No. 11, 1880-1881 (1958).

[19] B. M. Vul, J. Tech. Phys. (U.S.S.R.) **25**, No. 1, 3 (1955).

[20] B. M. Vul Радиотехника и электроника (Radio Engineering and Electronics) **1**, No. 8, 1040 (1956).

[21] J. O'Connel and L. J. Giacoletto, RCA Rev. **17**, No. 1, 68 (1956).

[22] A. Uhlir, Proc. IRE **46**, No. 6, 1099 (1958).

[23] Proc. IRE **47**, No. 3, 241A (1959).

[24] A. Uhlir, Bell Sys. Tech. J. XXXVII, No. 4, 951 (1958).

[25] B. Salzberg and E. W. Sard, Proc. IRE **46**, No. 6, 1301 (1958).

[26] H. Heffner and K. Kotzebue, Proc. IRE **46**, No. 6, 1301 (1958).

[27] Herrmann, Uenohara, and Uhlir, Proc. IRE **46**, No. 6, 1301 (1958).

[28] T. J. Bridges, Proc. IRE **46**, No. 2, 494 (1958).

[29] R. Adler, Proc. IRE **46**, No. 6, 1300 (1958).

[30] E. O. Keizer, RCA Rev. **18**, No. 4, 475 (1957).

[31] V. I. Samoĭlenko and I. A. Glotov (News of the Colleges, Radio Engg.) **2**, No. 1, 38 (1959).

[32] H. Shul, Phys. Rev. **106**, 384 (1957).

[33] M. T. Weiss, Phys. Rev. **107**, 317 (1957).

[34] A. L. Mikaélyan Радиотехника и электроника (Radio Engineering and Electronics) **3**, No. 11, 1323 (1958).

[35] IRE WESCON Convention record, part 3, 1958.

Translated by J. G. Adashko